Artificial neural network structure optimisation for accurately prediction of exergy, comfort and life cycle cost performance of a low energy building

Iván García Kerdan*, David Morillón Gálvez

Instituto de Ingeniería, Universidad Nacional Autónoma de México, 04510 Ciudad de México, México

Abstract

In recent years, surrogate modelling approaches have been implemented to overcome the time and computational power demands of traditional building energy modelling. Artificial neural networks (ANN), due to their potential to capture building energy systems complex interactions are regarded as powerful surrogate models; however, the definition of optimal ANN structures and hyperparameters have been overlooked causing substandard prediction performance. The aim of this study is to present a novel hybrid neuro-genetic modelling framework developed as an open source tool capable of identifying optimal multi-input/multi-output ANN structures for accurately predicting building thermodynamic performance. The ANN optimisation process uses a genetic algorithm that minimises the root mean squared error (RMSE) data difference between the target and predicted values for both the training and testing data. As a case study, an archetype social house located in different climatic regions in Mexico is used. The ANN training database has been generated by simulating a sample of high-resolution energy models considering a combination of different active and passive energy strategies (input data) while calculating building exergy destructions, occupant thermal comfort and life cycle cost (output data). After automatically evaluating thousands of different structures, the neuro-genetic tool has identified a single deep ANN structure (3 hidden layers with 18, 17, 20 neurons respectively) capable of predicting the model's high output variability, achieving a prediction accuracy >0.95 for each of the outputs. The presented framework and tool can be adapted to further optimisation stages in the building design process and to solve similar problems in other research areas.

Keywords: exergy, artificial neural network, genetic optimisation, surrogate modelling, low-energy buildings

* Corresponding author
Email address: IGarciaK@iingen.unam.mx (Ivan Garcia Kerdan)

Nomenclature

A_b	total building area [m^2]
A_{col}	solar collector area [m^2]
$A_{PV/T}$	hybrid photovoltaic/solar collector area [m^2]
CC_n	capital cost [US$]
CE_n	annual energy cost [US$]
e	euler's number [e = 2.718]
E_{PV}	PV electricity generation [kWh]
$En_{dem,th}$	zone thermal energy demand [KWh]
En_{light}	artificial lighting energy demand [kWh]
En_{vent}	ventilation energy demand [kWh]
$Ex_{a/g}$	air or ground exergy [kWh]
$Ex_{dem,bui}$	total building exergy demand [kWh]
$Ex_{dem,th}$	zone thermal exergy demand [kwh]
$Ex_{dest,nonren}$	non-renewable exergy destructions [kWh]
Ex_{DHW}	domestic hot water exergy demand [kWh]
Ex_{light}	lighting exergy demand [kWh]
$ExDU_{nonren}$	exergy destructions intensity [kWh/m^2]
$Ex_{sup,nonren}$	non-renewable exergy supply [kWh/m^2]
$Ex_{sup,tot}$	total exergy input supply [kWh]
Ex_{sun}	solar exergy input [kWh]
Ex_{vent}	ventilation exergy demand [kwh]
F_p	primary energy factor [-]
F_q	fuel quality factor [-]
G	incident solar radiation [W/m^2]
L	thermal load [W/m^2]
M	metabolic rate [W/m^2]
M_n	maintenance cost [US$]
Q_{col}	solar collector energy generation [kWh]
Q_{DHW}	hot water energy demand [kWh]
Q_{gen}	building thermal systems primary energy consumption [kWh]
q_{fuel}	energy source quality factor [-]
r_d	discount factor [-]
T_0	outdoor temperature [K]
$T_{a/g}$	air or ground source temperature [K].
T_i	inside setpoint temperature [K]
T_{op}	operational temperature [°C]
$T_{p_{WH}}$	hot water demand average temperature [K]
T_{sun}	sun temperature [K]
W_{hp}	heat pump electricity demand [kWh]

Greek Symbols

η	system energy efficiency [-]
ψ	system exergy efficiency [-]

Acronyms

ANN	Artificial neural network
ANN-GA	Hybrid neuro-genetic algorithm
ASHP	Air-source heat pump
COP	Coefficient of performance

ELM-WT	extreme learning machine with wavelet transform algorithm
GA	Genetic algorithm
GP	Gaussian process
GSHP	Ground-source heat pump
LHS	Latin hypercube sampling
MAE	Mean Absolute Error
NSGA-II	Non-dominated sorting genetic algorithm II
ORC	Organic Rankine cycle
PMV	Predicted mean vote index
RBF	Radial basis function
RLC	reinforcement leaning control
RMSE	Root mean square error
SVM	Support vector machine

1 Introduction

Globally, buildings are responsible for approximately 20-40% of the national primary energy utilisation [1] and 25-30% of the global CO_2 emissions [2]. In recent years, the international community has committed to reduce emissions from the building sector and according to the International Energy Agency [3], energy efficiency has been regarded as the first fuel to achieve a sustainable global sector holding the largest cost-effective potential among decarbonisation measures.

As the challenge of improving energy and resource utilisation in the building sector is becoming more evident, developing techniques for designing sustainable, efficient and cost-effective buildings and energy systems is still a challenge that researchers, engineers and architects face nowadays. Commonly, there has been a reliance on complex dynamic simulation tools to assess the environmental performance of buildings and to optimise energy and resource utilisation [4]. Pre-processing efforts and running the optimisation process are regarded as major limitations due to the nature of detailed building modelling and the expensive computational cost [5]. However, in recent years, driven by the focus of reducing computational times, this research area has moved from using complex dynamic simulation and optimisation tools to relying more on data-based and machine learning solutions [6]. Specifically, surrogate modelling using non-parametric models such as artificial neural networks (ANN), support vector machines (SVM), and Gaussian process models (GP) have been the most popular methods used in design, sensitivity and uncertainty analysis and optimisation of building energy systems [7].

In addition, automated machine learning (AutoML) techniques have been developed recently. Regularly, AutoML is employed during the design and development phase to automatically select machine learning algorithms, thus, assisting inexperienced users in developing their own machine learning models. Barreiro et al. [8] developed the Net-Net AutoML approach to test different model typologies to predict complex Biological Ecosystems Networks. Similarly, Feurer et al. [9] developed *auto-sklearn*, an AutoML Python package that uses Bayesian optimisation to automatically improve machine learning models performance by taking into account previous performance of similar datasets. Nevertheless, the main limitation for more experienced users is the inherited constraints of such black-box frameworks, limiting the flexibility in adapting new features. Furthermore, the application of such frameworks in building energy design has been limited.

Apart from the computational aspect, other research groups have focused on improving applied thermodynamic analysis [10]. In this sense, exergy analysis have found some space among the research community aiming at improving energy utilisation in buildings [11]. This method derives from Thermodynamics' 2nd Law principles in combination with the 1st Law. The main advantage of exergy analysis compared to traditional energy analysis, is the identification of exact locations of irreversibilities

or true inefficiencies, which in buildings mostly occur in thermal energy exchange processes and in the delivery of high quality energy sources (electricity, gas) to cover low quality demands (cooling heating and hot water). From a sectoral perspective, using resources inefficiently and unwisely have a considerable effect on the national energy system and energy security [12]. However, if these irreversibilities (exergy destructions) are minimised, then high-exergy or high-quality energy vectors can be re-oriented to cover higher quality processes such as high-temperature heat demand in the industrial and chemical industry or electricity demand for the transport sector.

Thus, this study aims to integrate highly efficient computational algorithms with novel thermodynamic methods to ultimately improve the prediction capability and support design decisions for low energy buildings. This paper is organized as follows. First, the most relevant literature about exergy and machine learning applications in building research is presented. Secondly, the proposed methodological framework and case study are described. The presented approach combines dynamic exergy analysis modelling with a hybrid AutoML approach, more specifically, an Artificial Neural Network-Genetic Algorithm (ANN-GA) process, which aims at optimising complex ANN structures to improve prediction performance. As an added value, the ANN-GA algorithm is presented as an open source tool with further development potential by the research community. Following, the paper shows the application of the framework using a social house building model located in Mexico. First, using data from building energy simulations as training and testing data, optimal ANN structures are identified via the proposed framework. Secondly, the section shows the optimised ANN model prediction performance of the output targets, namely building exergy destructions, thermal comfort and life cycle cost. Finally, conclusions and suggestions for future work are presented.

2 Literature review

2.1 Building exergy analysis

Entropy minimisation and exergy methods, which act as complement of common energy analysis, have been applied for more than three decades in areas such as cryogenics [13], industrial processes [14], air separation [15], combustion [16] and power generation [17], eventually reaching certain degree of maturity. The application of the Thermodynamics' 2nd law overcomes 1st law limitations by explicitly defining locations, causes, and magnitudes of energy deterioration [18]. By locating the sources of these inefficiencies, designers, engineers or decision makers can make more informed decisions aiming at minimising exergy destructions as much as possible.

Gasparatos et al. [19] demonstrated the intrinsic low thermodynamic efficiency of current buildings recommending further exploration of the causes. In building research, efforts have been made to develop consistent exergy analysis methods, such as the ones developed by the IEA-ECB Annex 49 [20] and the

'LowEx - COSTeXergy' [21] research groups. An updated review of the latest building exergy studies and developed methodologies can be found in [11]. However, as current building energy programmes and regulations still focus on maximising building envelope thermal performance, the application of exergy analysis, which hold the greatest potential in improving the performance of the building energy system, has been limited to academic work. In this sense, Fisk [22] criticized the low influence of exergy analysis on professional practice with very limited consideration in building construction guides and standards.

The limitations of using only the 1st Law in building energy design can be seen in other areas such as simulation and optimisation. In this regard, García Kerdan et al. [23] demonstrated that by using the 1st law only in the simulation and optimisation design process can limit the potential of obtaining the maximum possible thermodynamic efficiency in a building, evidencing that using both laws becomes a satisfactory approach to design more sustainable buildings. The study showed that by implementing exergoeconomic analysis, the building design optimisation process was able to achieve solutions with greater emissions' reductions compared to the typical energy approach, due to the capability of the former of locating and quantifying exact sources and locations of thermodynamic inefficiencies, being able to reduce them in a cost-effective way.

2.2 Surrogate modelling for energy design

In research and industry, building modelling has become a common approach in the design and optimisation of energy efficient buildings [5]. Commonly, complex simulation tools are used for this task. For instance, Shadram et al. [24] developed a physics-based multi-objective optimisation framework using Grasshopper, EnergyPlus and Octopus. In this case, to reduce simulation times in the parametric study, the building models needed to be simplified, reducing models' accuracy but dramatically improving computational power requirements. However, recently data-driven approaches, such as surrogate modelling, have been integrated more frequently aiming at reducing simulation times [7]. Surrogate models are statistical models that aim to approximate complex simulation models. In building design, such models are usually developed through machine learning methods, a common methodology in control research [25]. According to Geyer and Singaravel [25] the main steps to build and use a surrogate model in building energy design are the following:

i. Build a detailed simulation model.
ii. Run that model for many different cases to generate a database of results.
iii. Use the outputs to train and test the meta-model.

Surrogate models have the potential to be used as a rapid tool to support design decisions for building practitioners [26]; however, data quality needs to be assessed. Nonetheless, while the use of surrogate models has the capacity to ease computational burden and reduce simulation and post-processing times,

the time to develop the surrogate model needs to be carefully considered as it can greatly affect the design process.

Westermann and Evins [7] provided a comprehensive review of surrogate modelling application for building design and optimisation. In optimisation studies, surrogate modelling is used to accelerate the optimisation process and to enable gradient based approaches. However, as Hashempour et al. [27] argues, the greatest complexity lies in the selection of conflicting objectives. The study suggests the importance of implementing integrated decision-making models that have the potential to satisfy environmental and human comfort aspects such as thermal, visual and acoustic comfort.

Wortmann et al. [28] suggest that for general architectural design there is a faster convergence in surrogate-based optimisation than metaheuristic methods. Among surrogate-based optimisation techniques, typical linear regression models [29], Lasso regression [30], radial basis function (RBF) algorithms [31], and Support Vector Machines (SVM) [32] are commonly used; nevertheless, Artificial Neural Networks (ANN) were found to be the most popular method for surrogate modelling-based optimisation, with energy use, overheating, carbon emissions and total cost as the most common prediction outputs [7].

2.2.1 ANN for building energy design

ANN were first developed in the late 1950s aiming at simulating the neuron network behaviour of the human brain [33]. Similar to the regression model process, the ANN learns the relationship between the data inputs and the defined (controlled and uncontrolled) variables by analysing the previously and/or newly fed data. Detailed information on ANN theory can be found in Hagan et al. [34].

ANN has been applied in many academic fields, mainly those where modelling and prediction of engineering systems is necessary. In energy research, Kalogirou [35] was one of the first researchers to illustrate the potential of ANN for the design of a wide variety of energy systems. More specifically, in building energy design, Magnier and Haghighat [36] used a simulation-based ANN to characterise building behaviour. Then, the model was integrated with a multi-objective Genetic Algorithm aiming at minimising simulation times compared to classical optimisation approaches. Melo et al. [26] evaluated the feasibility of using an ANN to improve accuracy of simplified models for national labelling purposes. The ANN was applied to model the building stock of a Brazilian city based on the results of extensive EnergyPlus simulations. Sensitivity and uncertainty analyses were carried out to evaluate the behaviour of the ANN model, indicating that an ANN was able to represent with high accuracy the interaction between input and output data for a vast and diverse building stock.

Wong et al. [37], using hourly EnergyPlus simulations, developed ANN models aiming at improving energy use, thermal demand, and electric lighting for a building with high daylight potential. The obtained surrogate models were able to dynamically simulate the building as four of the inputs were directly related to the hourly climatic conditions found in the EnergyPlus weather file. Following, a simple optimisation exercise considering two of the nine input variables was conducted, aiming at finding the minimum electric lighting consumption. Similarly, Ascione et al. [38] applied a Multi-Layer Perceptron (MLP) ANN model to predict energy performance for new and retrofit building designs. The authors used two different families of ANN models to predict heating and cooling energy use, thermal comfort and electricity production from PV (exclusively for retrofit projects). The ANN models showed good prediction capability reducing computational times by 98%.

Although with limited application, ANN can be used to derive meta-models, overcoming the limitation of derivative-free optimisation algorithms [39]. Sharif and Hammad [40] aimed at reducing simulation times from physics-based multi-objective optimisation studies, implemented ANN surrogate models by using data from optimisation runs. The study focused on retrofit projects aiming at reducing total energy use, life cycle cost and carbon emissions of a university building. The surrogate-based optimisation method was able to reduce simulation times by up to 99%.

2.2.2 Exergy-based ANN studies

In the field of exergy analysis, some ANN studies can be found in the literature, but with limited application to buildings. Sözen and Arcaklioğlu [41] used ANN to obtain exergy losses of an ejector-absorption heat transformer. As these systems require complex differential equations and computational models, the application of ANN was able to dramatically reduce computational times while showing high statistical coefficient of determination compared to outputs from the complex model. Yoru et al. [42] applied a simplified ANN model to predict the exergy performance of a gas turbine. Outputs demonstrate good prediction performance of ANN models with Root Mean Square Error (RMSE) values below 0.002.

Khosravi et al. [43] used adaptive neuro-fuzzy inference system and ANN to model energy and exergy efficiency of a geothermal organic Rankine cycle (ORC) equipped with a solar thermal equipment. The developed model was built considering the main design parameters of the system such as solar radiation, well temperature, flow rates and pressures and solar collector area. Aghbashlo et al. [44] used extreme learning machine with wavelet transform algorithm (ELM-WT) to estimate the exergetic performance of a biodiesel/diesel engine. Compared to typical ANN models, the proposed approach was able to better predict thermodynamic performance with a Pearson coefficient of around 0.95.

Yang et al. [45] investigated the application of reinforcement leaning control (RLC) for low exergy building systems using different ANN structures. Using PV/T panels as case study, the authors found that the

proposed RLC method outperformed the typical rule-based control by increasing net power output by up to 11.5%. When the whole building was modelled, the RLC met 100% of the required heating demand compared to 97% from typical control. Nevertheless, no studies were found that optimise building exergy performance using any type of machine learning technique.

2.3 ANN structure optimisation

As shown, several studies have focused on producing ANN models capable of reproducing complex simulations results. Furthermore, some of these models have been applied for design optimisation; however, few energy publications have tackled the issue of finding optimal ANN structures as a measure to ensure that the best possible solution is obtained. Typically, this has been tackled using heuristic trial-and-error methods, limiting the number of studied structures. The main issue is that there is no general ANN structure that can be used for every problem, as it greatly depends on the problem and data type.

To tackle this limitation, neuro-evolutive algorithms have been proposed to train ANNs. This is mostly done through genetic algorithms combined with artificial neural networks (ANN-GA). The first applications can be found in areas such as civil and structural engineering. Koopialipoor et al. [46] applied a hybrid ANN-GA to model the overbreak induced by the drilling in tunnel operations. Similarly, Azimi et al. [47] used a hybrid neuro-genetic approach to find optimal ANN structures to better predict blast induced ground vibrations due to mining. The optimal ANN structure shows higher prediction accuracy compared to empirical predictors and neuro-fuzzy system approaches.

In the field of combustion, Taghavi et al. [48] implemented a neuro-genetic approach to optimise three different ANN structures: Autoregressive Networks, MLP and RBF. The application of genetic algorithms ensured that optimum structures were found for each type of network. For instance, when comparing the prediction capability of the optimised MLP network against the conventional approach, the performance prediction was increased from 0.89 to 0.96 while also reducing the computational time for network training. Suresh et al. [49] coupled an ANN with GA optimisation to calculate the maximum possible efficiency of an ash coal power plant. Flow sheet simulations were used to train the ANN models. Following, using the ANN performance metrics as fitness function, the model found a set of optimal input parameters that resulted in minimum energy requirements and an increase in exergy efficiency. Finally, Baklacioglu et al. [50] used a ANN-GA, to optimally select the parameters of the network to model the exergetic efficiency of a turboprop engine. The authors utilised the momentum factor to improve the backpropagation algorithm to adjust the weight parameters of the ANN. The outputs suggest that the proposed hybridisation provides an increase in the accuracy and fitness of the results.

2.4 Research gap

For building energy research, the literature review has shown a limited amount of studies focusing on the application of exergy analysis and enhanced machine learning techniques for rapid and effective prediction of sustainable and thermodynamic efficient buildings. Although a wide range of studies and simulation tools oriented to assess building exergy design seem to be in place, no efforts have been made to combine it with ANN modelling. Conversely, ANN structure optimisation, which has only been applied to specific research areas, have failed to provide generalisable open source tools and methods for application, limiting its research scope to a single field and probably a single study.

This paper proposes a novel development of an exergy-based ANN model to accurately predict energy/exergy performance and other metrics such as occupant thermal comfort and life cycle cost. However, to ensure that the best prediction model is obtained, a genetic optimisation is applied to discover the best possible ANN structure and hyperparameters. To ensure reproducibility and generalisation of the proposed framework, the programming code is presented and published as an open source collaboration software.

3 Materials and methods

The proposed exergy-based neuro-genetic framework is shown in Fig.1 and can be summarised in the following steps:

1. *Building energy/exergy baseline simulation model development*. In this step, a detailed building energy model is thermodynamically evaluated using ExRET-Opt [51], a recently developed building simulation tool based on the EnergyPlus engine [52] that further integrates exergy and exergoeconomics analyses.
2. *Parametric study design and simulation.* Considering different building energy technologies and measures, a near-random sample is generated using Latin Hypercube Sampling (LHS) method and simulated using ExRET-Opt. The aim at this stage is to generate a comprehensive database that would be used to train the ANN.
3. *ANN training and surrogate model development*. With the database in place, the neuro-genetic tool based on Python-based machine learning libraries is adopted to train the ANNs using backpropagation. Although build upon a limited amount of simulated results from dynamic thermal simulations (step 2), the framework allows the ANN to learn the complex thermodynamics interactions between the building physics and the building energy systems.
4. *ANN structure optimisation.* At this stage, genetic optimisation is applied to find optimal ANN hyperparameters and structures preserving the essential behaviour of more complex modelling configurations. The optimisation process can define as a cost function different ANN performance metrics such as RMSE or MSE.

5. *Optimised ANN prediction performance.* After the optimal ANN structure is identified by the tool, prediction performance against the physics-based energy modelling target outputs is conducted.

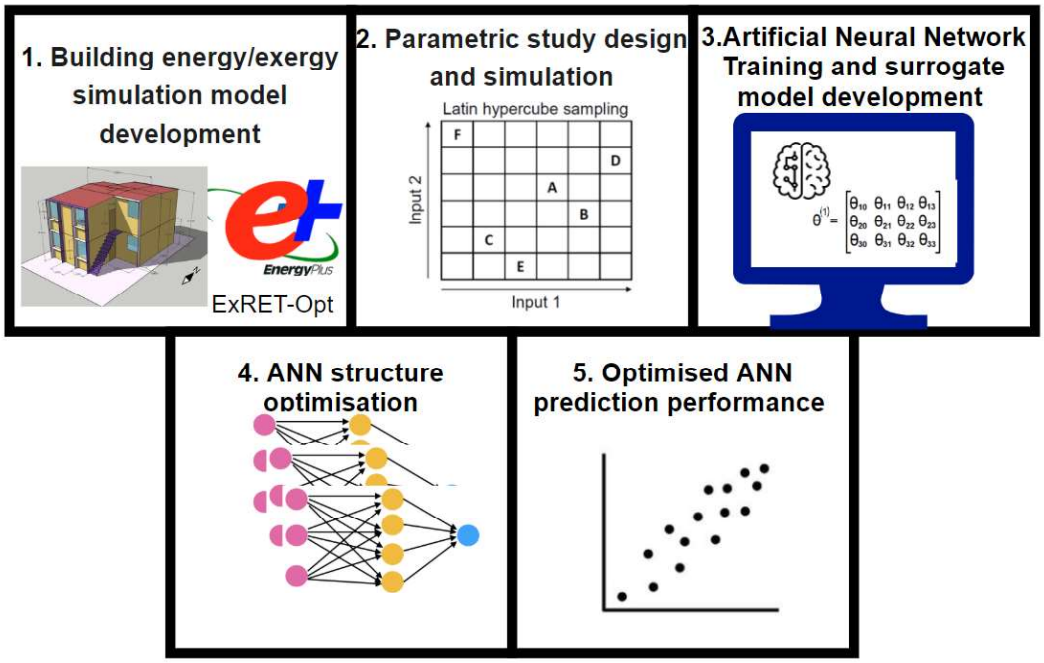

Fig. 1 Poposed exergy-based hybrid neuro-genetic framework for ANN structure optimisation

3.1 Mathematical modelling: Exergy, LCC and thermal comfort

This section presents a general overview of the main mathematical formulas employed to obtain the desired prediction outputs: i) exergy destructions, ii) life cycle cost, and iii) thermal comfort. These have been integrated and modelled into the energy/exergy simulation tool (ExRET-Opt) described in Step 1 in the previous action. More detailed information about the formulas [51], tool's technical description [53] and applications [54] can be found.

3.1.1 Exergy analysis

As mentioned, exergy analysis is integrated to locate the main sources of irreversibilities in the energy system. This study considers an input-output exergy analysis that requires a thermodynamic abstraction of energy subsystems located in the building. The section presents a simplified version of the analysis applied in this research. The detailed calculation and thermodynamic abstraction of building energy systems can be found in [55].

As first step, it is necessary to calculate the total exergy demand of the building. This will represent the minimum exergy required to cover all services. In this study, following four demands have been considered:

i. Thermal exergy demand (heating and cooling)

$$Ex_{dem,th}(t_k) = \sum_{i=1}^{n} \left(En_{dem,th}(t_k) * \left(1 - \frac{T_0\,(t_k)}{T_i\,(t_k)}\right)\right) \quad \text{[kWh]} \tag{1}$$

where T_0 is the outdoor temperature [K], T_{ith} is the inside setpoint temperature [K] and $En_{dem,th}$ is the thermal energy demand [kWh].

ii. Ventilation exergy demand

$$Ex_{\,vent}(t_k) = \sum_{i=1}^{n} \left(En_{vent}(t_k) * \left(1 - \frac{T_0\,(t_k)}{T_i\,(t_k) - T_0\,(t_k)} ln \frac{T_i\,(t_k)}{T_0\,(t_k)}\right)\right) \quad \text{[kWh]} \tag{2}$$

where $En_{\,vent}$ is ventilation energy demand.

iii. Domestic hot water exergy demand

$$Ex_{DHW}(t_k) = Q_{DHW}(t_k) * \frac{\eta_{WH}(t_k)}{q_{fuel}} * \left(1 - \left(\frac{T_0(t_k)}{T_{p_{WH}}(t_k) - T_0(t_k)}\right) * \ln\left(\frac{T_{p_{WH}}(t_k)}{T_0(t_k)}\right)\right) \quad \text{[kWh]} \tag{3}$$

where Q_{DHW} is the hot water energy demand [kWh], η_{WH} is the system efficiency [-], q_{fuel} is the energy source quality factor [-], and $T_{p_{WH}}$ is the hot water demand average temperature [K].

iv. Lighting exergy demand

$$Ex_{light}(t_k) = En_{light}(t_k) * F_q \quad \text{[kWh]} \tag{4}$$

where En_{light} is the energy demand for artificial lighting [kWh], and F_q is the fuel quality factor [-], in this case electricity (1.0). Other end-use services such as refrigeration and cooking have not been considered in this study. Thus, to obtain the total building exergy demand:

$$Ex_{dem,bui} = Ex_{dem,th}(t_k) + Ex_{\,vent}(t_k) + Ex_{DHW}(t_k) + Ex_{light}(t_k) \quad \text{[kWh]} \tag{5}$$

The detailed analysis calculates the exergy flow through the rest of the subsystems. For instance, for the HVAC systems this means calculate exergy flows in the emission, distribution, storage, generation and supply systems [51]. On the other end, it is necessary to calculate the total exergy supplied to the building. This serves to assess the overall exergy destructions and exergy efficiency of the entire building. Although exergy analysis does not differentiate exergy destructions depending on the energy source, for this study, a distinction has been made between non-renewable and renewable-based exergy inputs. This has been done to encourage the application of renewable energy-based technologies. Thus, for non-renewable-based exergy, the followed equation is used:

$$Ex_{sup,nonren}(t_k) = \sum_i \left(\frac{Q_{\,gen,i}(t_k)}{\eta_{gen,i}\,(t_k)} * F_p * F_q\right) + \left(Ex_{light}(t_k) * F_p\right) \quad \text{[kWh]} \tag{6}$$

where, Q_{gen} is the primary energy consumption by the building thermal systems (HVAC and DHW systems) [kWh], η_{gen} is the systems' energy efficiencies [-], F_p [-] is the primary energy factor [56], F_q is fuel quality factor [20], and Ex_{light} is the lighting exergy demand [kWh].

For renewable-based exergy inputs, the formulas proposed by Torío et al. [57] have been implemented. In this study, solar, air and ground energy have been considered as renewable sources. For instance, equipment using solar energy, such as solar collectors, the exergy input is calculated considering the production and the collectors' efficiency. Thus, solar exergy input (Ex_{sun}) can be calculated as follows:

$$Ex_{sun}(t_k) = G(t_k) * A_{col} * \left(1 - \frac{T_0(t_k)}{T_{sun}}\right) \quad \text{[kWh]} \tag{7}$$

where G is the incident solar radiation [W/m^2], A_{col} is the area of the solar collector [m^2] and T_{sun} is the source temperature (~6000 K). In the presence of a photovoltaic generation, exergy efficiency ($\psi_{PV/T}$), and consequently exergy inputs, can be calculated as follows:

$$\psi_{PV/T} = \frac{E_{PV}(t_k) + Q_{col}\left(1 - \frac{T_0(t_k)}{T_{in}(t_k)}\right)}{G(t_k) A_{PV/T}\left(1 - \frac{T_0(t_k)}{T_{sun}(t_k)}\right)} \quad \text{[-]} \tag{8}$$

where $E_{PV}(t_k)$ is the electricity generated through the PV panels [kWh] and Q_{col} is the thermal energy generated by the solar collector [kWh]. In this case, the denominator represents the total solar exergy input into the system. On average, considering typical energy efficiencies for both technologies, a hybrid PV/T has an exergy efficiency of around 13% [57].

The study also considers heat pumps to cover thermal energy demands, specially cooling and domestic hot water demand. Therefore, the energy located in the air or the ground is also considered as renewable exergy inputs. To calculate the exergy efficiency of a heat pump (ψ_{hp}) and consequently the exergy input, the following formula can be used:

$$\psi_{hp} = \frac{Ex_{dem,th}(t_k)}{Ex_{a/g} + W_{hp}} = \frac{COP\left(1 - \frac{T_0(t_k)}{T_{in}(t_k)}\right)}{1 + (COP - 1)\left(\frac{T_0(t_k)}{T_{a/g}(t_k)}\right) + W_{hp}} \quad \text{[-]} \tag{9}$$

where Ex_g is ambient exergy (air or ground) [kWh], W is the heat pump electricity demand [kWh], COP is the heat pump coefficient of performance [-], and $T_{a/g}(t_k)$ is the source temperature [K].

Then, to calculate total exergy input supply ($Ex_{sup,tot}$), non-renewable and renewable exergy supply are added:

$$Ex_{sup,tot} = Ex_{sup,nonren}(t_k) + G(t_k) A_{PV/T}\left(1 - \frac{T_0(t_k)}{T_{sun}(t_k)}\right) + \left(1 + (COP - 1)\left(\frac{T_0(t_k)}{T_{a/g}(t_k)}\right) + W_{hp}\right) \quad \text{[kWh]} \tag{10}$$

As we are interested in calculating only exergy destructions from non-renewable sources, the following outputs, namely non-renewable-based exergy destructions and the total exergy destructions intensity $ExDU$ have been defined as follows.

$$Ex_{dest,nonren}(t_k) = Ex_{sup,nonren}(t_k) - Ex_{dem,bui}(t_k) \quad \text{[kWh]} \quad (11)$$

$$ExDU_{nonren} = \frac{Ex_{dest,nonren}}{A_b} \quad \text{[kWh/m}^2\text{]} \quad (12)$$

where A_b is the total building area [m^2]. Eq. 12 represents the first of the three output values considered in the simulations and used to train the ANN models.

3.1.2 Life cycle cost (LCC) analysis

The second output, which is life cycle cost (50 Years), is calculated as follows:

$$LCC = \sum_{n=1}^{N} \frac{[CC_n + M_n] + [CE_n]}{(1+r_d)^n} \quad \text{[US\$]} \quad (13)$$

where n is the total years of evaluation (in this case 50 years has been selected), CC_n is the design's capital cost [US$], M_n is the maintenance cost [US$], CE_n is the annual energy cost [US$] and r_d is the discount rate [-].

3.1.3 Thermal Comfort

The third output, thermal comfort has been calculated considering two different metrics depending if the building is mechanically or natural ventilated. For mechanical ventilated designs, the Predicted Mean Vote (PMV) index is used to account for total hours of discomfort. PMV is a result of Fanger's comfort equation [58] by developing a correlation with the thermal loads. By providing a quantitative combination between individual and environmental variables, PMV will indicate the occupants' judgement of the climatic conditions. Detailed information on the derivation of PMV can be found in [59] and is calculated as follows:

$$(|PMV|) > 0.5 = |(0.303e^{-0.036M} + 0.028)L| > 0.5 \quad [\text{ - }] \quad (14a)$$

where M is the metabolic rate [W/m^2], L is the thermal load [W/m^2], and e is the Euler's number [e = 2.718]. If the PMV is greater than 0.5, this considers that the space is providing uncomfortable period.

For natural ventilated designs, the adaptive comfort model is used [60]. This model considers the effect of outdoor temperature on the indoor environment conditions. The main difference with the PMV model, is that outdoor conditions dynamically affects the comfort zone, usually assuming that occupants are more tolerant to a wider temperature range. The comfort temperature is defined as follows:

$$T_{op} = 0.31 * T_0 + 17.8 \pm 2.5 \qquad [°C] \qquad (14b)$$

where T_{op} is the average between the indoor air dry bulb temperature and inside surfaces mean radiant temperature [°C] while T_0 is the outside temperature [°C]. Any temperature outside the range will be considered as uncomfortable conditions. Both metrics (14a) and (14b) are calculated by ExRET-Opt using the EnergyPlus engine. As the model considers an hourly resolution, the discomfort hours are aggregated at an annual level to then convert it to annual percentage time of thermal discomfort.

3.2 Building case study and parametric study

The case study building model is based on a two-storey/two-flat social house located in Mexico (Fig. 2). This design has been used in a previous study by the authors where the calibration and validation process have been conducted [54]. In Table A-1 (Appendix A), the baseline envelope and energy system technical details are presented.

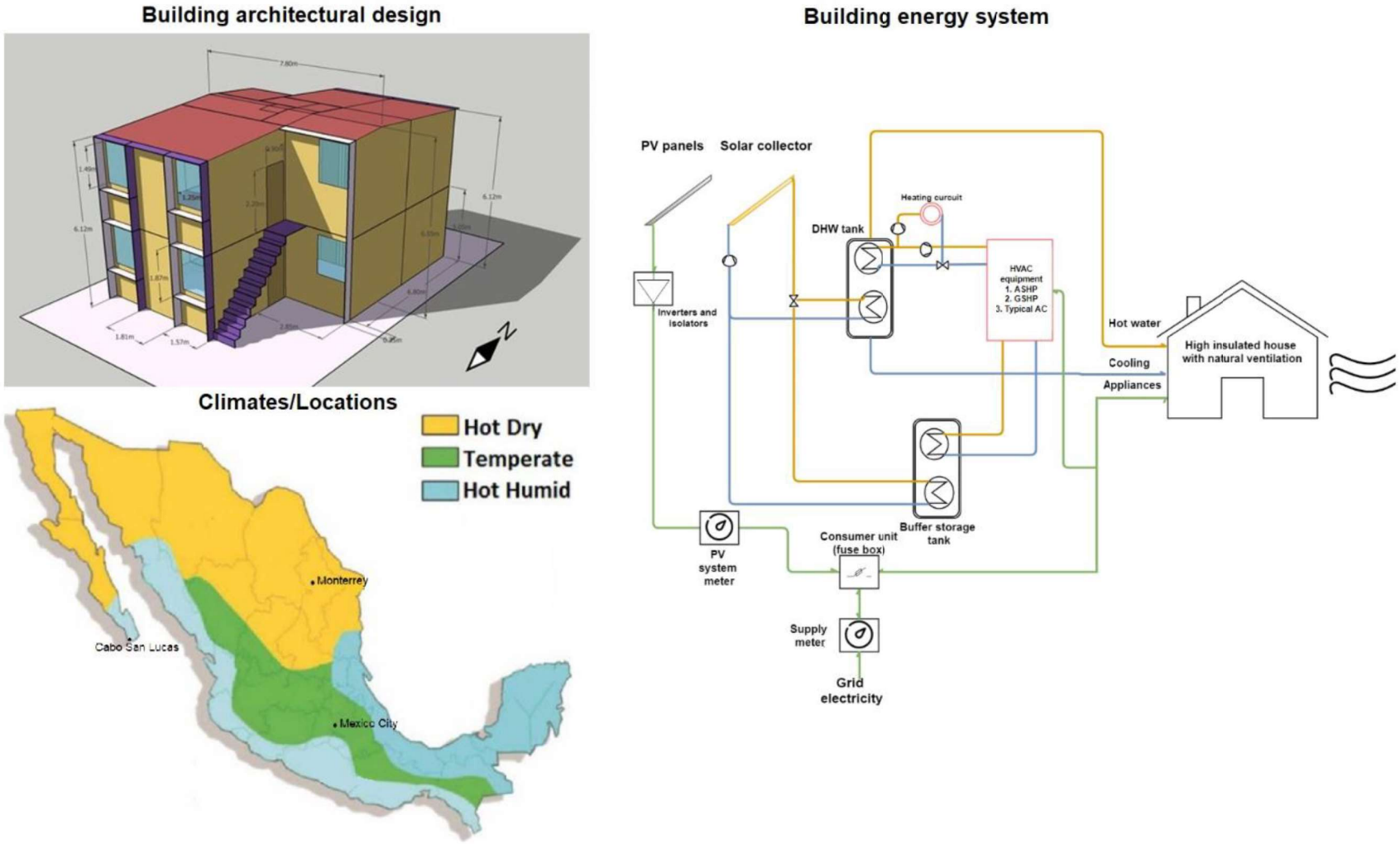

Fig. 2 Archetype duplex social house layout, baseline energy system schematic and considered locations

To assess different building designs, the study considers a wide range of passive and active technologies. Among the possible measures that can be modelled are diverse insulation types and widths, glazing systems, solar protection devices (overhangs and fins), artificial lighting devices as well as renewable technologies such as solar PV, solar collectors and micro wind turbines. Regarding the HVAC system, the model considers either using natural ventilation or the option between an air source heat pump (ASHP) or ground source heat pump (GSHP). As an added complexity, this study has also considered as input variables three different locations, representing Mexico's three main climates (Fig. 2). Detailed technical and economic information of all possible design parameters (climate, passive and active technologies) that would also act as input variables in the database generation and consequently ANN training process can be found in Table 1, resulting in a search space of around 6.8 quintillion different solutions.

To generate the database sample, a parametric study has been conducted using Latin Hypercube Sampling (LHS), where 3,000 different building models are simulated. LHS has been selected as sampling method as it stratifies the input probability distributions, assuring an even spread of sample data points across the search space. The size of the database represents only $6e^{-16}$ % of the total search space; however, it is expected that the proposed framework is capable of finding robust ANN models even with limited amount of data. The physics-based models have been set with an hourly resolution, meaning that 8760 outputs for each desired variable are simulated for each model. As the physics-based modelling tool (ExRET-Opt) has the capability to perform sizing calculation for any equipment, this enables the automatically generation not only of the design's operational energy/exergy expenditure but also the project's life cycle cost (eq. 13). The entire simulation and database generation process required a computational effort of 72 hours using an Intel Core i5 8 GB PC. This generated data can be found in the Supplementary Information (S.1).

As shown in Table 1, the ANN design will consider a total 21 parameter. This is a significant simplification, as the amount of inputs that can be found in the physics-based model are hundreds or even thousands of different variables. Thus, the aim was to create efficient ANN models that capture the complexity of physics-based simulation while still providing reliable outputs similar to those from the dynamic energy/exergy simulation tools.

Table 1 Technical and economic characteristics of input data for database generation

Input ID #	Type Technologies/ measures	Subtype Technologies/ Measures	Description	Cost unitary/range [US$]
1	Weather data	n/a	1.1 Hot-humid climate: • Cabo.San.Lucas.Intl.AP.767503_TMYx.epw 1.2 Hot-dry climate: • Monterrey-Escobedo.Intl.AP.763943_TMYx.epw 1.3 Temperate climate: • Ciudad.Mexico-Juarez.Intl.AP.766790_TMYx.epw	n/a
2	HVAC System	• Air source heat pumps + Variable Air Volume (VAV)	HP COP: 2.5 and 3.0 1.2 Single duct VAV with cooling efficiency of 75%	600-800 US$ / kW + 930 US$ per VAV system
		• Ground source heat pumps + Variable Air Volume (VAV)	HP COP: 3.5 (horizontal boreholes) Single duct VAV with cooling efficiency of 75%	1600 US$ / kW + 930 US$ per VAV system
3	Cooling setpoint	n/a	Values: 20 to 25 °C, with 0.1 °C resolution	n/a
4	Building orientation	n/a	Values: 0 and 360° with respect to the North, with 10° resolution	n/a
5-13	Solar protection (per window)	• Overhangs • Fins	Material: PVC module with 20 mm width Length values: 0.05 to 2.0 m	40 US$/m^2
14	Glazing	• Single	5mm clear glass (U_v = 5.7 W/m^{2}K)	130 US$/m^2
		• Double	5mm clear glass with a 6/13 mm gap (air, argon or krypton) (U_v = 1.2-1.3 W/m^{2}K)	350-500 US$/m^2
		• Triple	5mm clear glass with a 6/13 mm gap (air, argon or krypton) (U_v = 0.8-0.9 W/m^{2}K)	620-870 US$/m^2
15 **16**	Wall Insulation* Roof Insulation	• Polyurethane	2 to 15 in 1 cm steps	8.9-31.0 US$/m^2
		• Extruded polystyrene	1 to 15 in 1 cm steps	6.3-42.5 US$/m^2
		• Expanded polystyrene	2 to 15 in 1 cm steps	5.8-13.2 US$/m^2
		• Cellular Glass	4 to 18 in 1 cm steps	21.6-97.0 US$/m^2
		• Glass Fibre	6.7 7.5 8.5 and 10 cm	7.5-10.3 US$/m^2
		• Cork board	2 to 30 in 2 cm steps	7.4-114.1 US$/m^2
		• Phenolic foam board	2 to 10 in 1 cm steps	7.4-29.1 US$/m^2
		• Aerogel	0.5 to 4 in 0.5 cm steps	35.6-259.5 US$/m^2

		• Phase change material (PCM)	10 and 20 mm	76.8-143.3 US$/$m^2$
17	Air Gap	• Wall air gap	0 to 15 in 1 cm steps	n/a
18	Lighting	• CFL lamps	Low wattage lamps with low ballast factor. Power density: 10.5 W/m^2	150 US$/kW
		• LED	Low wattage solid-state lamps. Power density: 3.5 W/m^2	300 US$/kW
19	Solar photovoltaic	• Solar PV panels	Monocrystalline silicon panels with module efficiency of 13%	850 US$/$m^2$
20	Solar thermal	• Solar collectors	Flat plate solar thermal collector (HSTC) with 70% efficiency.	38 US$/$m^2$
21	Wind energy	• Wind turbines	Small scale wind turbines (micro) 1.0 - 1.5 kW	1000-3000 US$ per unit

3.3 ANN definition for surrogate model

The main advantage of using ANNs over other machine learning techniques, is the ability to learn more efficiently complex interrelated parameters by ignoring non-significant variables and data. This has the potential to develop more efficient models that could be easier to optimise. The basic ANN structure is made of an input layer, hidden layer(s), and an output layer.

The structure of the ANN has been set as a multilayer perceptron (MLP), which is a feed-forward neural network with one or more layers between the input and output layers and where backpropagation is used as a supervision learning method. When designing an MLP, the main issue is to determine the number of layers and neurons. The neurons are made of three characteristics: 1) one or more weighted input connections, a transfer function, and one or more output connections.

As mentioned, in this study the input layer is made of 21 different inputs (Table 1) including climate data, insulation material, the HVAC system, PV/T panels, etc. Conversely, the output layer consists of three nodes representing exergy destructions (eq. 12), life cycle cost (eq. 13) and thermal discomfort (eq. 14a or 14b). Although the physics-based model was based on hourly simulations providing a time-series resolution for each of the three outputs, these outputs have been aggregated annually for both exergy destructions and life cycle costs. Similarly, for thermal discomfort, where the physics-based model

provides a time-series of discomfort hours, these results have been converted to a percentage time of annual discomfort, resulting in three annual output variables that are handled by the ANN. The process will then specify an aleatory number of hidden layers and nodes between the input and output layers (Fig. 3).

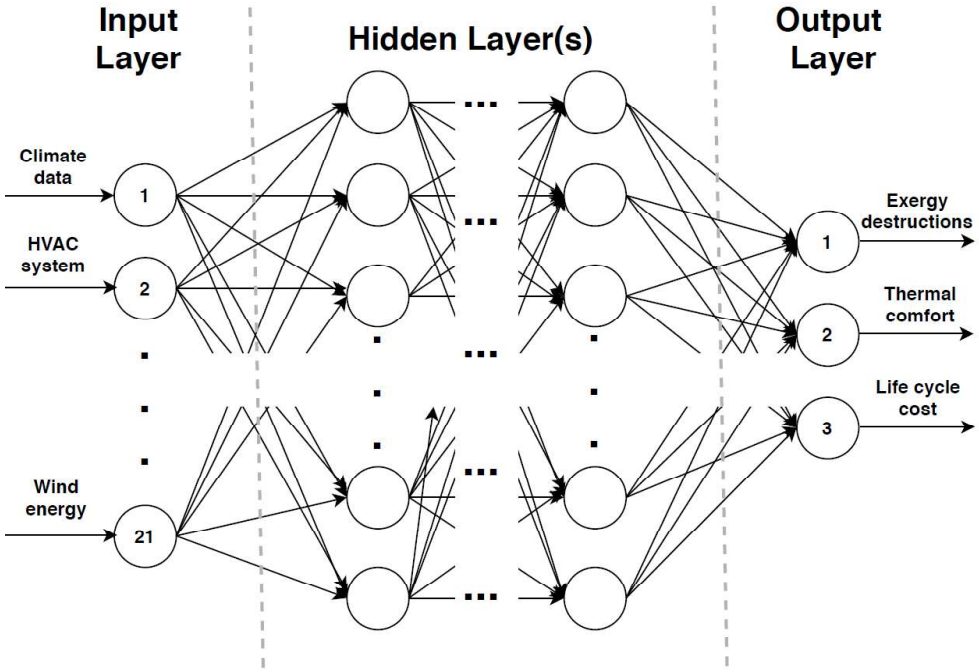

Fig. 3 Feed forward MLP ANN model structure

In an MLP, the outputs are recommended to be scaled. The scaling provides a more stable training procedure by reducing the gradient size used to update the weights. Also, it is important to understand the ratio between the number of input parameters and the amount of available data. The amount of data needs to be large enough to have a regulation effect and avoid the risk of overfitting and other undesired noise when generating the model.

3.4 ANN structure optimisation

Although the use of ANN has provided with several benefits in different research areas, the ANN structure and hyperparameters definition are problem-dependant. ANN hyperparameters can be catalogued as external parameters set by the network user. The selection of these will have important implications in the ANN performance, where the optimal combination of these is not a trivial task.

Normally, the design process of ANN structures is based on a trial and error approach, mostly driven by the experience of the user. To automate the process, it has been suggested to include a genetic optimisation procedure, allowing the exploration of a multidimensional space of possible structures. In this study, the design of the MLP ANN networks is done by integrating `TensorFlow` [61] and Python-based `Keras` [62] neural network libraries into the presented tool. The selection of `Keras` allows the tool

for rapid development capable of efficient computational times and parallelism. To find optimal ANN structures, the recombination of the following hyperparameters has been considered:

- **Training/Testing Data Share**: [95/5, 90/10, 85/15, 80/20, 75/25, 70/30]
- **Number of Layers:** [1, 2, 3, 4]
- **Min/Max Number of Neurons per Layer:** [1:20]
- **Batch List:** [10, 25, 50, 100, 200]
- **Optimisers:** [`adam, adagrad, rmsprop, sgd`]
- **Kernel/weight Initialiser:** [`uniform, normal`]
- **Epochs:** [50, 100, 150, 200]
- **Dropout Rate:** [0.0, 0.1, 0.2, 0.3, 0.4, 0.5]
- **Activation Type:** [`relu, elu, tanh, sigmoid`]

Brute-force search represents the combination of 1,843,200 different ANN structures. Depending on the complexity of the ANN, it could take between 1 and 90 seconds to simulate each structure. In a best-case scenario, this could take at least 21 days to simulate all possible combinations. For the training/testing data share, the training share refers to the amount of data that will be used for fitting (or training) the model by adjusting the desired parameters, while the testing data will be used to understand the accuracy of the analysed ANN structure. The number of iterations, epochs and batch size are regarded as the parameters that mostly affect simulation times. Basically, these parameters affect the rate at which samples are fed for model training. The epochs represent the group of samples which are forward passed to the model to then backpropagate determining the optimal network weights.

To avoid overfitting, different dropout rates have been considered. A dropout rate refers to the probability *p* of each neuron within the network of not being considered during the training process (except in the output layer). Also, different activation functions have been considered providing non-linear complex functional mapping between inputs and output variables. This feature is what differentiates ANN from a linear regression model. For detailed information on the hyperparameters' characteristics, we advise the reader to visit the `Keras` documentation (https://keras.io/guides/).

As previously detailed, a Non-dominated Sorting Genetic Algorithm-II (NSGA-II) [63] is used to optimise the ANN structure. NSGA-II is one the most popular algorithms used in building design optimisation and renewable energy implementation research [64]. The main advantaged of using NSGA-II is to reduce the probability of local minimum optimisation of the ANN structure. The complete neuro-genetic optimisation framework is illustrated in Fig. 4. It shows a snapshot of the ANN structure optimisation process at each iteration. In each generation the networks with the highest score are selected to recombine and by using the classic GA operators of crossover and mutation, a new generation of improved networks are created.

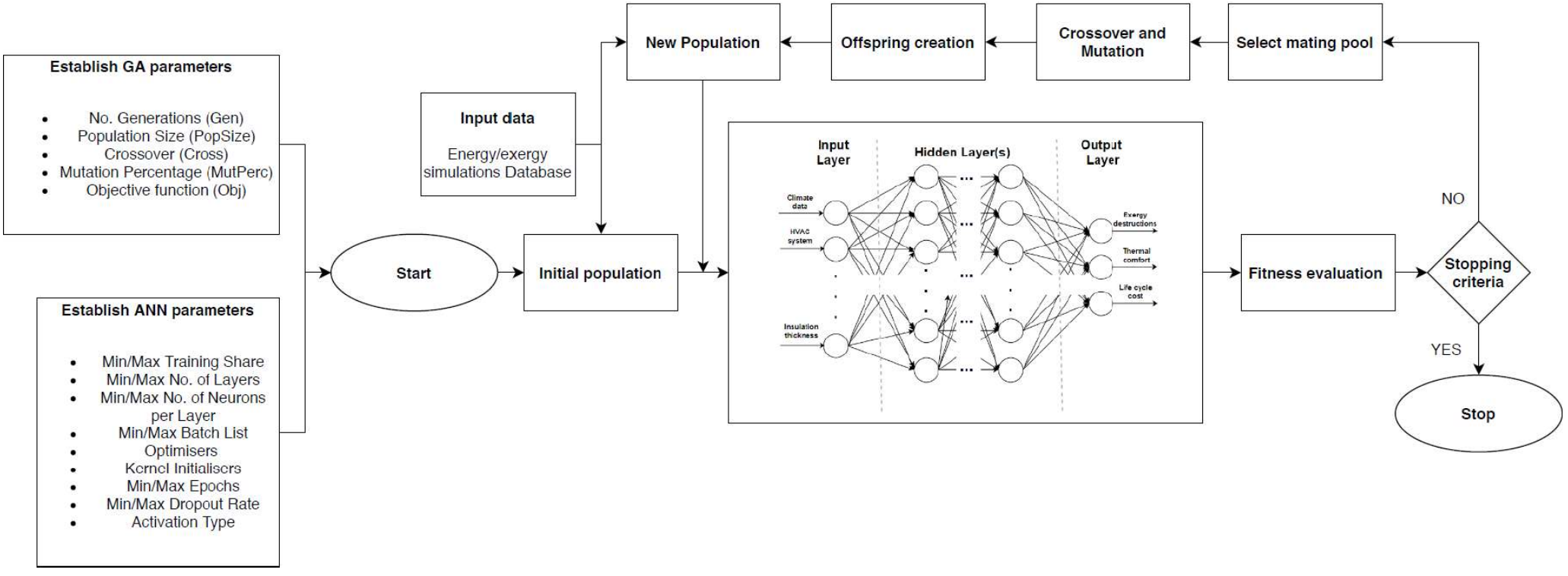

Fig. 4 Combined steps of the hybrid ANN-GA framework for neural network structure optimisation

3.4.1 Fitness Evaluation

The ANN training process will assign appropriate weights between the input layer and the immediate hidden layer, between the intermediate hidden layers (if any), and between the preceding hidden layer and the output layer. Different metrics can be used as fitness function to search for optimal ANN structures; however, this is not a trivial decision when the ANN is used to predict non-linear models. In this study, similarly to Perera et al. [65], Root Mean Square Error (RMSE) has been selected as fitness metric. The RMSE is a quadratic scoring rule able to measure the average error magnitude. In this case, the RMSE represents the error of the analysed ANN against the results from the physics-based simulation. The advantage is that it heavily penalises high errors, which is particularly desired in this study.

$$RMSE = \sqrt{\frac{1}{n}\sum_{j=1}^{n}\left(y_j - \hat{y}_j\right)^2} \tag{15}$$

where y_j is the j[th] actual value, $\hat{y}_j$ the j[th] predicted value and n the data number. The lowest RMSE at each generation for both the training and testing will determine the mating pool and chromosome selection that eventually would create the following generation. In this study, the objective function has been set as the average of the sum of the RMSE for both the training ($RMSE_{train}$) and testing ($RMSE_{test}$) data.

$$\min_X f(x) = \frac{RMSE_{train}+RMSE_{test}}{2} \tag{16}$$

3.4.2 Source code

The presented neuro-genetic framework for ANN structure optimisation has been developed as an open source tool coded in Python [66]. The latest release has been archived in Zenodo (doi: 10.5281/zenodo.3893600). For development purposes, the source code has been made available in the following GitHub repository: https://github.com/kerdan85/NeuroGeneticExergy. For simplification, Table 2 shows the pseudocode of the complete ANN-GA optimisation process described in this section.

Table 2 Neurogenetic framework pseudo code

Start ANN-GA process *(main_Neurogenetic.py*)
- Import libraries (`tensorflow, Keras, sklearn, pandas`)
- **Define GA parameters**
  - No. Generations (Gen: 50)
  - Population Size (PopSize: [10,20,30,40,50])
  - Crossover rate (Cross: 20%)
  - Mutation Percentage (MutPerc: 50%)
  - Objective function (Obj: Eq. 17)
- **Define ANN parameters range**
  - Min/Max Training Share: [95/5, 90/10, 85/15, 80/20, 75/25, 70/30]
  - Min/Max No. of Layers: [1, 2, 3, 4]
  - Min/Max No. of Neurons per Layer: [1:20]
  - Min/Max Batch List: [10, 25, 50, 100, 200]
  - Optimisers: [`adam, adagrad, rmsprop, sgd`]
  - Kernel/weight Initialisers: [`uniform, normal`]
  - Min/Max Epochs: [50, 100, 150, 200]
  - Min/Max Dropout Rate: [0.0, 0.1, 0.2, 0.3, 0.4, 0.5]
  - Activation Type: [`relu, elu, tanh, sigmoid`]
- **Generate Initial Population of ANN models for g=1**
- **Genetic Algorithm Started *(genetic.py)***
  - for *g*=1 to Gen:
    - while termination condition not met:
      - for *i*=1 to PopSize:
        - **Exergy/Comfort/LCC Dataset Import *(data_input.py)***
          - Define Train and Test data for population *i*
          - **Artificial Neural Networks Modelling (*ann.py*)**
            - Initialise `keras`
            - Define network (layers, neurons, etc.)
            - Compile network
            - Fit and evaluate network
            - Make predictions
            - Metrics outputs (e.g. `RMSE, MAE`)
        - **Generation *g* solutions list**
        - **Fitness evaluation of Generation *g***
          - Select the best parents in the population for mating
          - Generating next generation using crossover
          - Variations to the offspring using mutation
          - Creating the new population based on the parents and offspring
          - Generate Population of ANN models for *g+1*
- **End Genetic Algorithm**
- **Rank of best solutions and define best ANN structure**
- **Optimal ANN structure Performance Evaluation**

End ANN-GA process

4 Results and Discussions

4.1 ANN structure optimisation

With the building energy/exergy database in place (Section 3.2), five different genetic optimisation procedures have been conducted. Before proceeding, first, it was of interest to determine the optimum population size (*PopSize)* per generation. Population size is a genetic algorithm parameter and not of the ANN structure. Thus, the following PopSize = [10,20,30,40,50] have been considered. Fifty generations have been assigned as the stopping criteria considering the fitness value (Eq. 17) as objective function.

Fig. 5 (left), shows the convergence of each of the simulations. Results show that a population size of 40, which converges after the 26th generation, provides the best performance; while a PopSize=10 resulted with the worst performance. Fig. 5 (right), illustrates the best fitness and mean fitness values at each generation specifically for the PopSize=40 simulation.

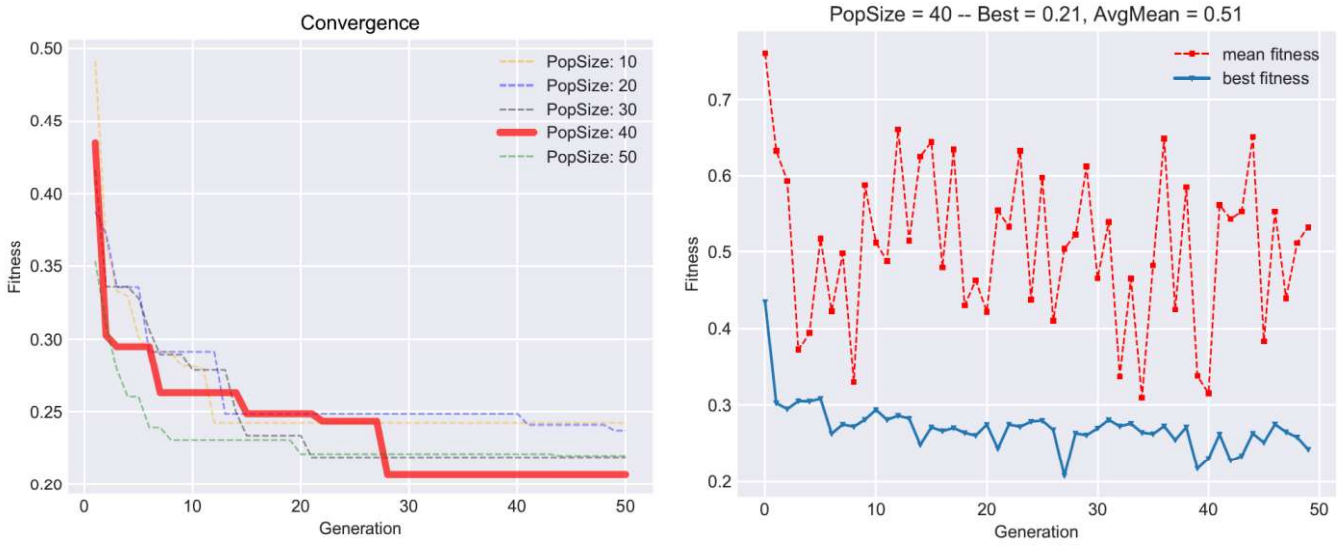

Fig. 5 Convergence and fitness evaluation considering different population (left) sizes and fitness performance for PopSize = 40

Table 3 summarises the overall performance and optimal ANN structure obtained for each population size simulation. For instance, considering a PopSize= 10, the optimisation has converged more rapidly locating a shallow ANN structure (1 hidden layer with 18 neurons) resulting in the worst overall fitness performance. On the other hand, results show that while the population size increases, deeper optimal networks are found by the genetic algorithm with an increase in fitness value and coefficient of determination (R^2) performance by 3.5% and 1.1% respectively.

Table 3 Top ANN model performance for different population sizes

	Generation	Layers	Neurons	R^2	$RMSE_{train}$	$RMSE_{test}$	Fitness (Objective)
PopSize=10	11th	1	18	0.959	0.203	0.282	0.243
PopSize=20	48th	2	20, 20	0.961	0.198	0.277	0.237
PopSize=30	20th	2	18, 20	0.968	0.180	0.258	0.219
PopSize=40	27th	3	18, 17, 20	0.970	0.173	0.242	0.208
PopSize=50	43rd	3	19, 18, 10	0.964	0.190	0.251	0.220

Usually, it is expected that the greater the population size the greater the possibility that the initial populations will have the optimal solution; however this can also cause an increase in generations for convergence as there is an increase in the occurrence of mutations; therefore more generations are necessary to get rid of undesired mutations. By setting a limited amount of generations (50) in this study, the optimal size is represented by a mid-population number with an increased accuracy. That is the reason why a PopSize of 40 and 30 have a better convergence performance than a PopSize=50, as sometimes midsized populations will show lower variations in fitness values. The detailed outputs for every PopSize simulation can be found in the Supplementary Data (S.2). In this section, only the data obtained from PopSize=40 is further analysed as it provided the best fitness value. In this simulation, the total evaluated ANN models were 2,000. On average, the time required to train each model was 20 s.

Fig. 6 and Fig. 7 shows the fitness performance summary for two specific ANN hyperparameters: epochs and the training/testing share. For the former, the graphs show the results obtained between epochs magnitudes (50, 100, 150, 200) with respect to the number of layers and optimiser type. A trend seems to appear showing that structures with 2-3 hidden layers, high epoch size values (>150) while using the '*adam*' optimiser, provide the best performance. An interesting insight is that, although using an ANN structure with 3 hidden layers seems to provide slightly better results, higher variability was found when compared to models with 2 hidden layers, resulting in a higher mean value of the fitness function. A similar trend can be seen when focusing on the training/testing share parameter (Fig. 7). Overall, the results show that testing data shares between 20% and 25% with 1-2 hidden layers, provides better average outcomes; however, the optimisation process found the best solution using a share value of 30% with 3 hidden layers. This outcome highlights the strengths of the optimisation process on finding solutions outside the local minimum and that would be difficult to identify in a common trial and error approach. In Appendix B, similar plots for the rest of ANN hyperparameters (batch size, kernel type and dropout rate) can be found.

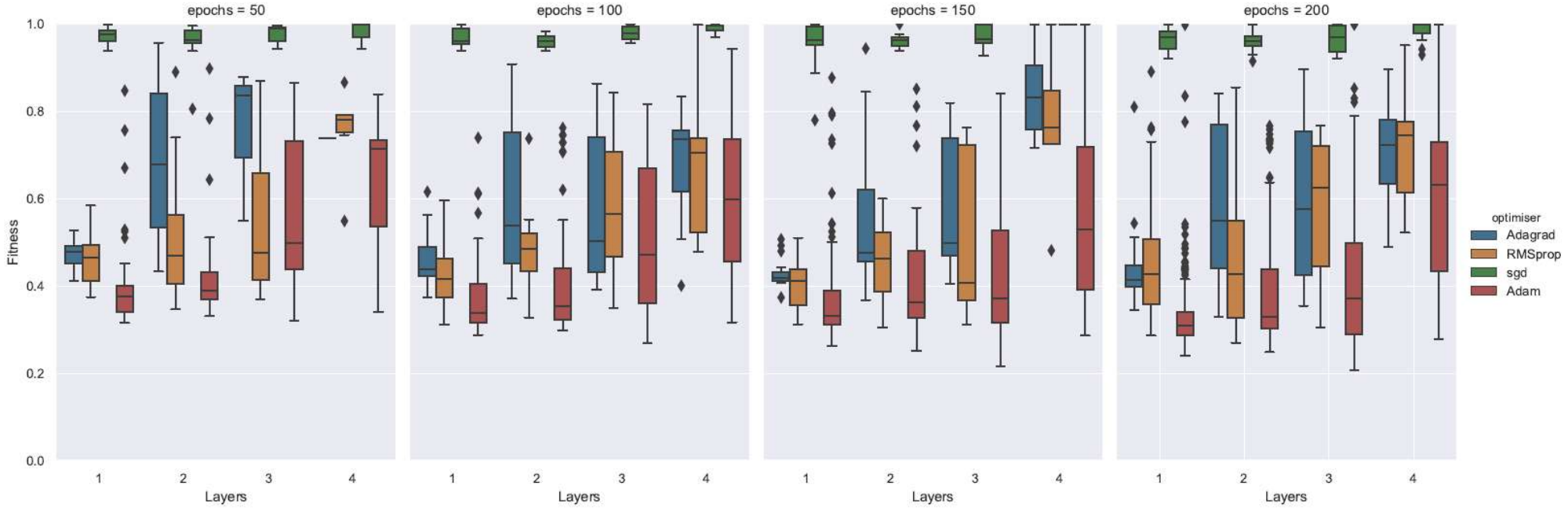

Fig. 6 Epochs hyperparameter fitness evaluation

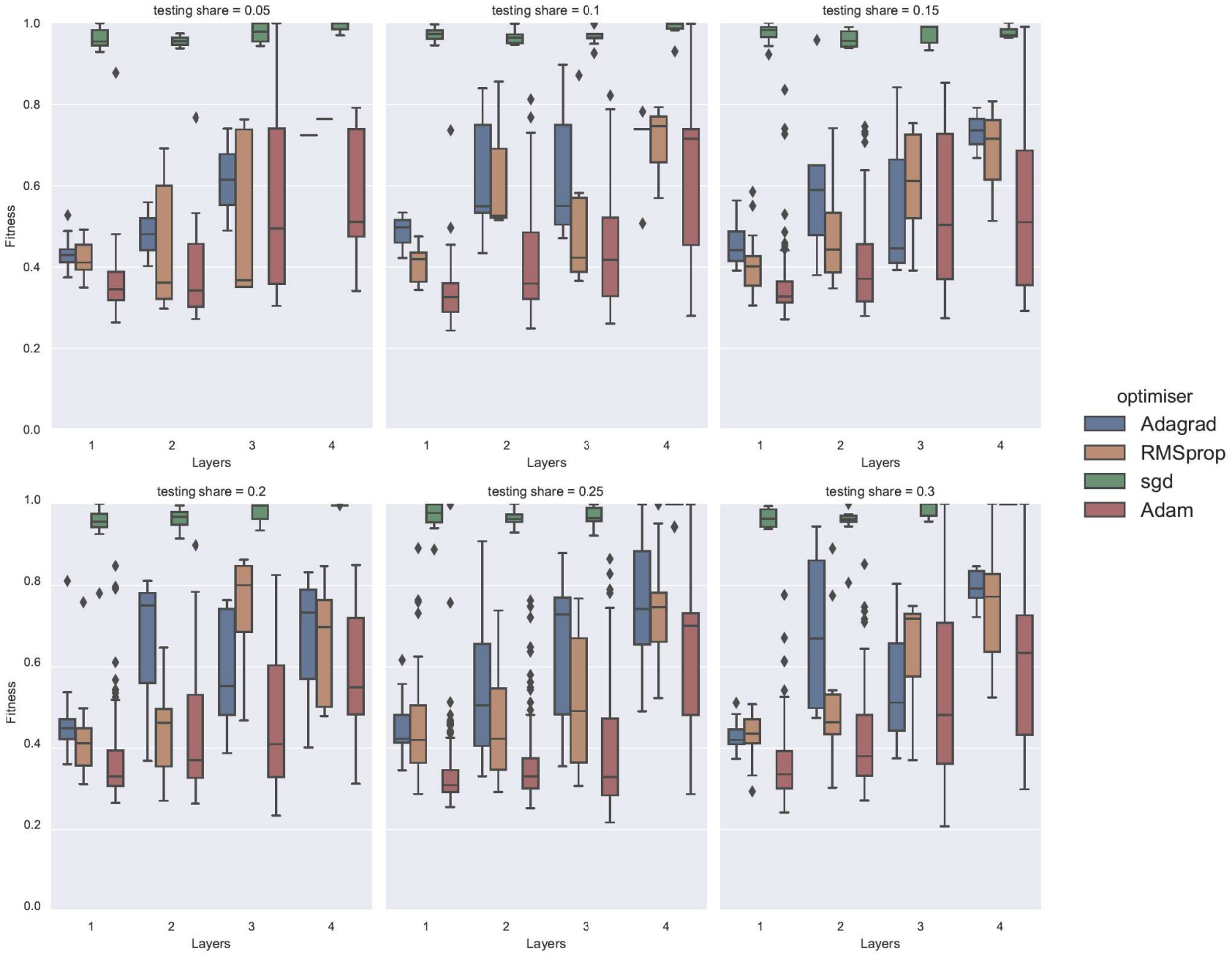

Fig. 7 Testing share hyperparameter fitness evaluation

Table 4 summarises the top ten ANN structures and hyperparameters based on the fitness value. The ANN structure with the best fitness (0.208) appeared in the 27th generation. The identified structure consists of 3 hidden layers with the following number of neurons [18, 17, 20] respectively. In terms of hyperparameters, the optimal training and testing data share has been found at 70/30. Also, the model considers a batch size and epochs at 10 and 200 respectively while using `adam` as an optimiser, `uniform` distribution as weight initialiser, and exponential linear unit (`elu`) as activation function.

Table 4 Top ten ANN structures and hyperparameters (Simulation PopSize = 40)

rank	generation – item #	hidden layers	neurons	batch	optimiser	kernel/ weight init.	epochs	dropout rate	test %	activation	$RMSE_{train}$	RMS_{test}	Objective
1	27-1081	3	(18, 17, 20)	10	adam	uniform	200	0	0.3	elu	0.173	0.242	0.208
2	31-1594	3	(20, 19, 8)	10	adam	normal	150	0	0.25	elu	0.182	0.252	0.217
3	31-1578	3	(20, 19, 8)	10	adam	normal	200	0	0.25	elu	0.188	0.267	0.228
4	33-1681	3	(20, 19, 8)	25	adam	normal	200	0	0.25	tanh	0.190	0.265	0.228
5	32-1601	3	(20, 19, 8)	10	adam	normal	200	0	0.25	elu	0.197	0.263	0.230
6	34-1724	3	(20, 19, 8)	10	adam	normal	200	0	0.2	elu	0.197	0.271	0.234
7	21-1093	1	20	10	adam	uniform	200	0	0.3	tanh	0.206	0.276	0.241
8	39-1963	3	(20, 19, 8)	10	adam	uniform	200	0	0.25	elu	0.193	0.292	0.243
9	16-841	1	19	10	adam	uniform	200	0	0.1	elu	0.214	0.274	0.244
10	32-1617	3	(20, 19, 8)	50	adam	normal	200	0	0.25	tanh	0.205	0.283	0.244

Considering the optimal ANN structure (rank =1), Fig. 8 shows the ANN training and testing performance by analysing the MSE and RMSE variation against the number of epochs. As illustrated, the MSE reaches a value of 0.045 (training) and 0.075 (testing) around epochs = 150 to then remain relatively constant, meaning a convergence in the model.

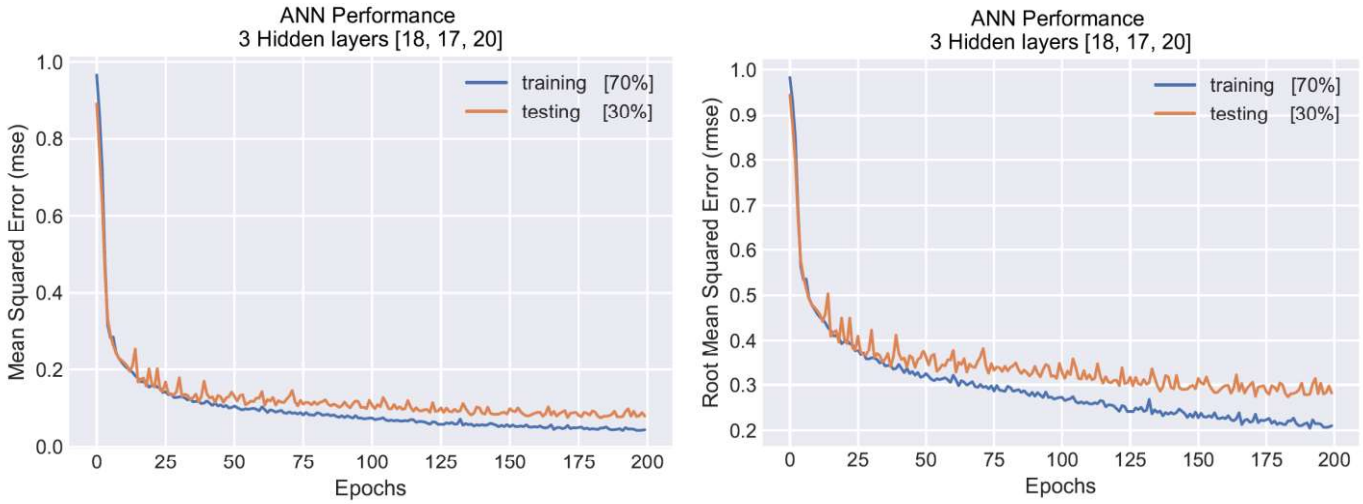

Fig. 8 MSE and RMSE performance for the optimal ANN model

4.2 Optimal ANN prediction performance

This section presents the output prediction performance of the identified optimal ANN model. Regression plots (Fig. 9) shows the non-renewable exergy destructions, thermal discomfort, and LCC correlation between the building physics-based model (ExRET-Opt) results or target values against the ANN model predictions. As shown, the optimised ANN (with a RMSE 0.173 and 0.242 for training and testing respectively), can predict more than 95% of the variance for the three different outputs. This is a very satisfactory outcome taking into account that the target data considers models with a diverse range of energy technologies located in three distinct climates. Usually, when a problem has multiple outputs, researchers tend to develop a family of ANN models to predict each single output. The advantage of the proposed optimisation procedure has shown the ability to identify a single ANN model capable of explaining multiple outputs with high variability.

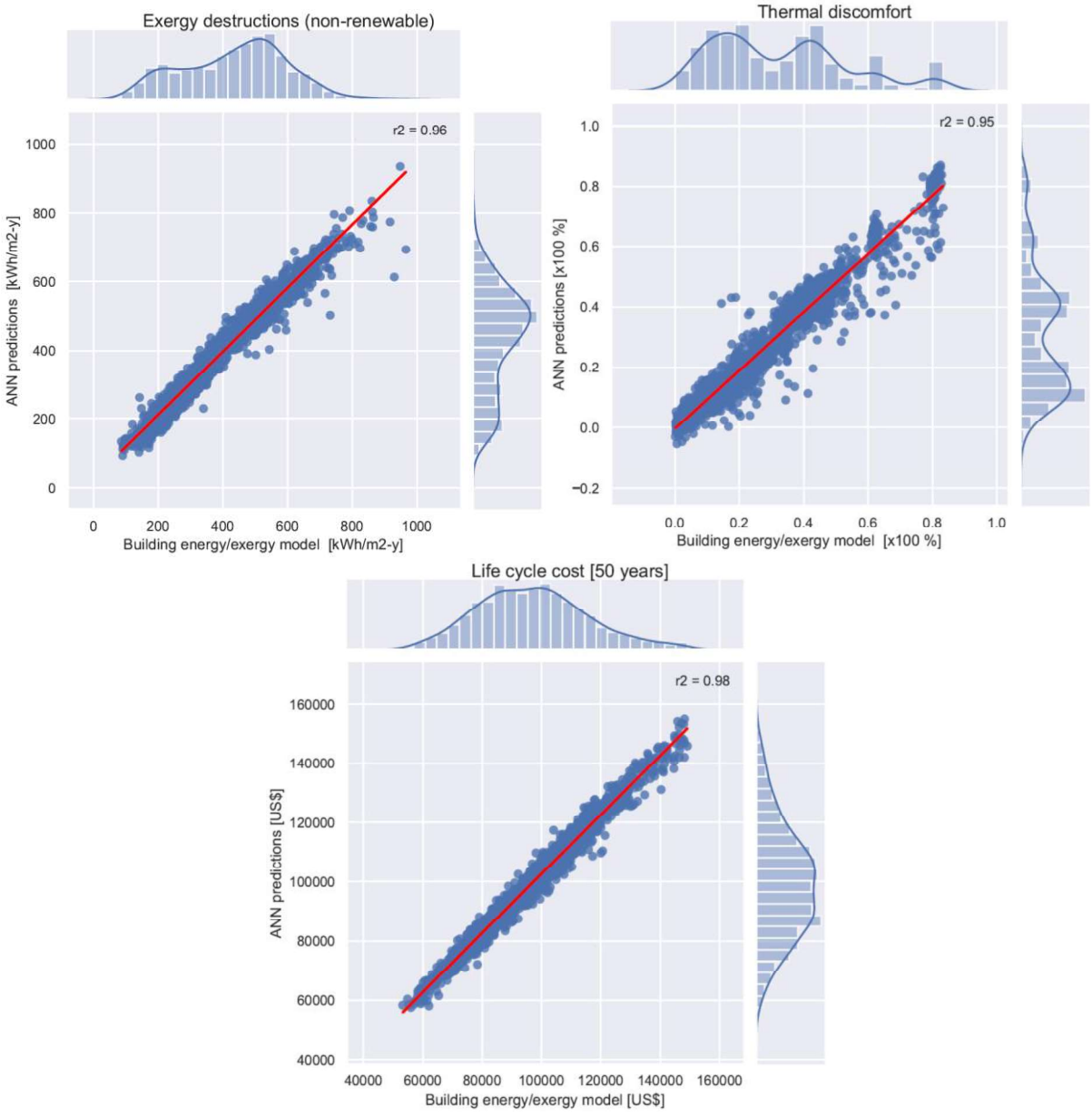

Fig. 9 Prediction performance of the optimal ANN model

Fig. 10 shows a comparison of the prediction error for each of the outputs. As shown, the normal distribution in each target output confirms the high reliability of the optimised ANN model in making predictions.

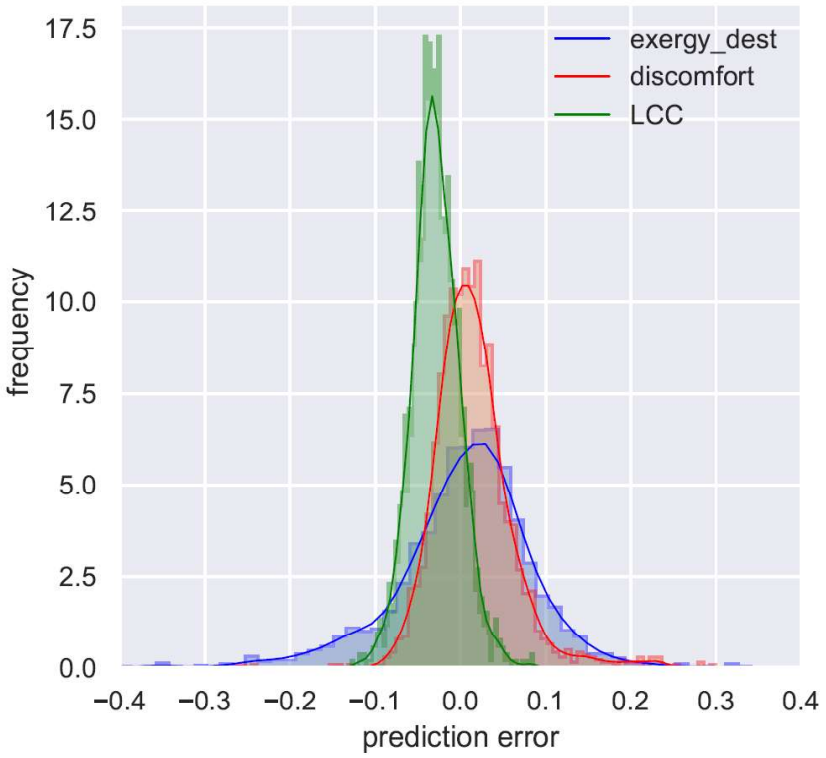

Fig. 10 Error histograms for prediction of exergy, discomfort and LCC using optimal ANN

To show the ANN model prediction capabilities of single models, Table 5 summarises the prediction error for four specific building designs: i) building model with the minimum exergy destructions, ii) building model with the minimum discomfort hours, iii) building model with the minimum life cycle cost performance and iv) equal weight Pareto solution building model.

Table 5 Performance prediction error for four building models

Model	ExRET-Opt physics-based model			Optimal ANN model prediction			Prediction error			
	Exergy Destructions [kWh/m^2-y]	Thermal discomfort [% hours]	LCC [$]	Exergy Destructions [kWh/m^2-y]	Thermal discomfort [% hours]	LCC [$]	Exergy Destructions [%]	Thermal discomfort [%]	LCC [%]	Average error (abs) [%]
minimum exergy destructions	**84**	62%	83,911	**117**	63%	83,756	-28%	-1%	0%	10%
minimum thermal discomfort	668	**0%**	83,240	614	**4%**	77,233	9%	-4%	8%	7%
minimum LCC	692	14%	**49,563**	639	22%	**47,614**	8%	-8%	4%	7%
Pareto (equal weight)	392	4%	75,221	387	13%	68,975	1%	-9%	9%	6%

4.2.1 Validation by climatic region

The main challenge for the developed ANN model has been to accurately predict building exergy destructions, comfort and LCC performance under different climatic conditions. Therefore, and for validation purposes, one hundred (100) building energy simulations for each climatic region have been conducted using the simple random sampling method.

For the specific case of the hot-humid climate, Fig. 11 illustrates the ANN model performance prediction against the target outputs as well as the associated residuals. These plots show the prediction, overprediction and underprediction by the optimal ANN model using a different set of data. The results illustrate that the model has been able to predict 94% of the overall variability of the new data. Considering the three outputs separately, LCC has been found to have the highest prediction performance (95%), followed by exergy destructions (94%) and discomfort hours (92%). Similar plots for the hot-dry and temperate climates can be found in Appendix C. Overall, by region, the ANN model has been found to have better prediction performance for the hot-humid region (94%), followed by temperate (94%) and hot-dry (93%) regions.

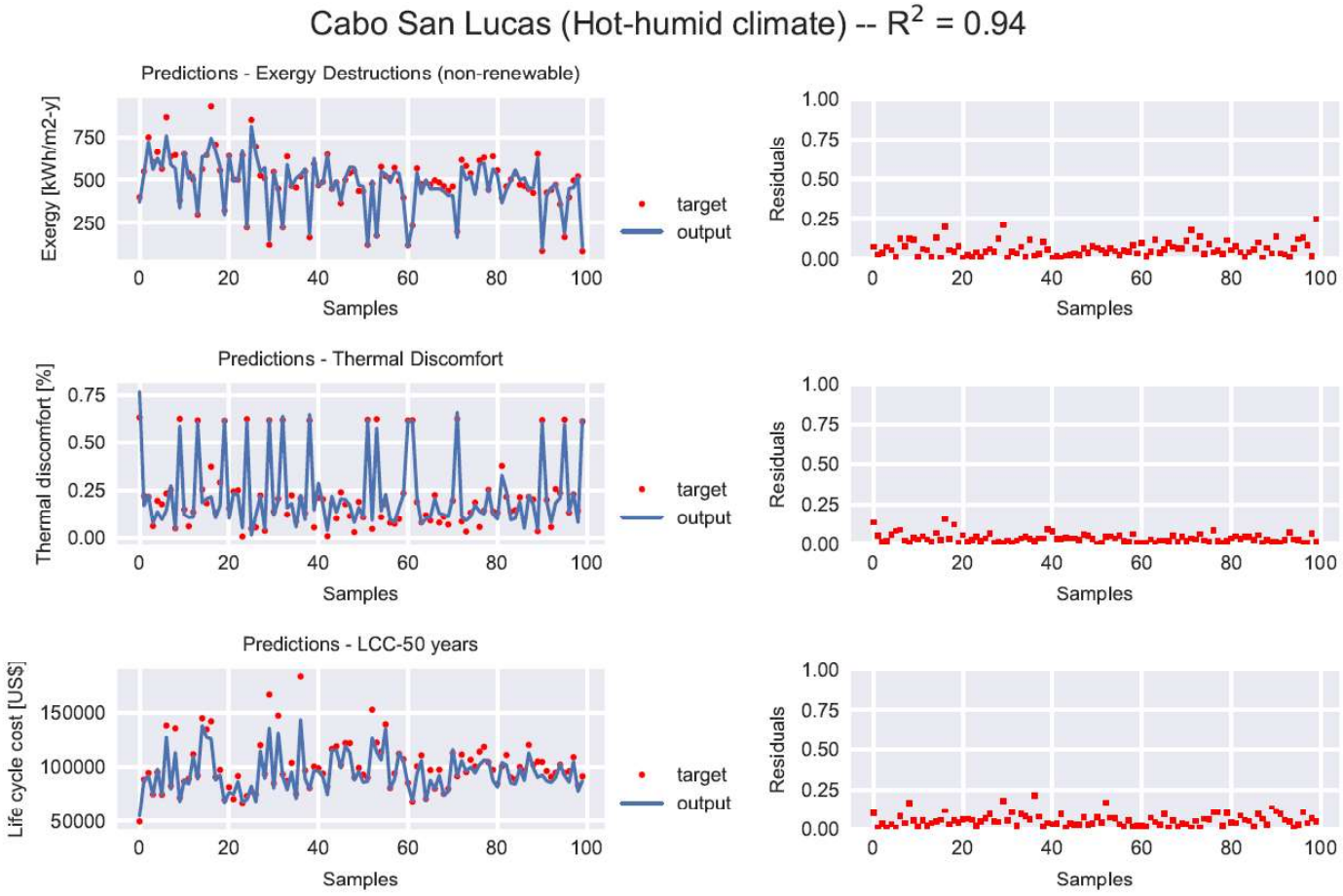

Fig. 11 Optimal ANN model prediction performance and residuals for exergy, comfort and LCC in hot humid climatic conditions

Table 6 summarises the relative absolute deviation distribution for each output and climatic region. Overall, LCC prediction has the lowest values of relative errors with 3.4%, 3.5% and 3.7% for the hot-humid, hot-dry and temperate climates respectively. Exergy destructions predictions has the highest errors due to model simplifications and complex thermodynamic interaction of the building energy system. This trend can be seen for every region, as almost 100% of thermal discomfort and LCC target values have been predicted within a <15% of average absolute error, while for exergy destructions, values have been predicted within a <25% range.

Table 6 Relative absolute error deviation distribution between the optimal ANN model and validation data

	Hot-humid (Cabos San Lucas, BCS)					
	R^2	**<1%**	**<5%**	**<15%**	**<25%**	**Average absolute errors**
Exergy destructions	0.94	13%	55%	94%	98%	6.0%
Thermal discomfort	0.92	12%	78%	98%	100%	3.9%
LCC	0.95	21%	76%	99%	100%	3.4%
	Hot-dry (Monterrey, NL)					
	R^2	**<1%**	**<5%**	**<15%**	**<25%**	**Average absolute errors**
Exergy destructions	0.92	8%	41%	87%	98%	7.7%
Thermal discomfort	0.93	11%	61%	93%	100%	5.3%
LCC	0.95	24%	76%	100%	100%	3.5%
	Temperate (Mexico City)					
	R^2	**<1%**	**<5%**	**<15%**	**<25%**	**Average absolute errors**
Exergy destructions	0.91	12%	55%	90%	97%	6.4%
Thermal discomfort	0.96	22%	77%	100%	100%	3.4%
LCC	0.94	17%	77%	98%	100%	3.7%

4.3 Discussion

The selection and development of surrogate models, and more specifically ANN models, for energy systems design is not a trivial task. Although normally this has been done as an iterative design process, where experience and knowledge have played a key role in its development, the probability of finding the optimal surrogate model structure is very low. The obtained results have highlighted the strengths of the proposed framework in identifying an optimal ANN model capable of accurately predicting complex performance variables. Furthermore, the integration of exergy analysis makes the framework suitable for identifying thermodynamic efficient building designs while keeping thermal discomfort and life cycle cost as low as possible.

The design variation of the case study building model by using different technologies and climatic conditions has generated high variability for each of the desired output; but more specifically, for non-

renewable exergy destructions. Due to the complexity of the case study, it was not expected that the optimisation procedure will identify shallow (single layer) networks as these are more suitable to represent linearly separable functions. On the other hand, multiple hidden layers can be used to represent convex regions. The identified optimal ANN structure, made of an input layer with 21 neurons (input data), 3 hidden layers with 18, 17, 20 neurons respectively, and an output layer with 3 neurons (output data), with very precise hyperparameters, would have been difficult to find if the proposed metaheuristics optimisation framework has not been applied. The identified optimal deep ANN model has been able to obtain an overall prediction accuracy above 95% and absolute errors below 8% for every output variable and climatic region. The study has shown that one of the key strengths of using the proposed hybrid neuro-genetic framework is the ability to define a single complex deep network that have the potential to predict multiple outputs with high variability.

Additionally, the results also have shown that parameters from the genetic algorithm might influence the identification of optimal ANN structure. In this study, only the population size has been varied with different ANN structure identification and prediction performances; nevertheless, we recommend that other metrics such as crossover rate or mutation to be varied as these could also have a considerable impact in the identification of optimal ANN structures. Among the ANN hyperparameters, low variability was found in the dropout rate. Apart from the dropout rate, batch normalisation is another well-recognised approach to avoid overfitting and reduce training time in multi-layer ANNs. Batch normalization can achieve significant training time reductions by normalising the input on each layer, allowing higher learning rates. As it also has a regularisation effect, it could make the use of the dropout rate redundant. According to Garbin et al. [67], each has its strengths and limitations and recommends to use them with caution. Nevertheless, it is recommended that batch normalisation to be implemented in future studies.

The developed approach ensures reproducibility and reliable predictions of energy/exergy performance, thermal comfort and LCC of any building design. Apart from saving computational time by bypassing the need to use EnergyPlus and ExRET-Opt for energy and exergy analyses, it provides a model with enough complexity to simulate different measures in different climatic locations. However, the study's main limitation is that the developed surrogate model has been trained using synthetic data, meaning that the accuracy highly depends on the data amount and generated quality as well as the characteristics of the dynamic energy/exergy simulation engine. Secondly, the selection of a single building design can limit to some extent the generalisation of the results, as different input data and possibly different ANN structures will be required for an accurate prediction performance. In this regard, the subjective selection of input variables could also have a significant effect on finding optimal ANN structures; however, while the addition of new input variables (neurons) to the input

layer could have a critical effect on the desired outputs, the framework has been developed and intended to be adaptable to other types of building designs, data types and even generalisable to other similar problems found in energy research.

5 Conclusions

This study has shown the development and application of a novel hybrid neuro-genetic (ANN-GA) framework for surrogate modelling structure optimisation. Although improvement in the required computational efforts and times is a common finding of such approaches, the study has also provided the capability to locate more efficient surrogate modelling structures by using the full potential of genetic optimisation. Furthermore, the paper has combined machine learning and exergy analysis, creating a new holistic and robust approach for the design of low-energy buildings. An important contribution of this study has been the publication of the framework/tool as open source, providing the research community with the capacity to improve and adapt the modelling framework accordingly.

In this study, data from 3,000 building models have been used to train and optimise ANN models. The optimisation process, which required the simulation of 2,000 different ANN structures, located an optimal solution by minimising the average sum of the RMSE for both the training and testing data. The optimal ANN model has been successfully applied and have provided accurate predictions for exergy, thermal discomfort and life cycle cost performance of a social house located in three different climates. One of the main advantages of the presented neuro-genetic framework, is that it allows the user to simplify the utilisation of surrogate models by using a single complex structure that can predict multiple outputs with high variability.

ANN structure optimisation also offers a robust approach for rapid identification of strategies and efficient designs for industry and policymakers. For the former, this will represent the reduction in time and power requirements, streamlining the design process and producing more exergoeconomic-efficient and environmentally friendly solutions. For the latter, the application of such framework could help identify national strategy solutions in different regions, aiding in developing sustainable building programmes and policies.

Although the focus of this paper was to automate the ANN structure procedure, a similar approach can be used to integrate a second optimisation stage to locate optimal building designs. This means that ongoing efforts to continue developing the open source tool are necessary. For future work, the research will focus on adding this feature to find optimal building design parameters that would optimise multiple thermodynamic and economic objectives.

Acknowledgements

The corresponding author acknowledges the support from 'Coordinación de la Investigación Científica' from the 'Universidad Nacional Autónoma de México' through a scholarship to pursue postdoctoral studies with a grant number: CJIC/CTIC/1011/2019.

References

[1] Pérez-Lombard L, Ortiz J, Pout C. A review on buildings energy consumption information. Energy and Buildings. 2008;40(3):394-8.
[2] IPCC. Fifth Assessment Report of the Intergovernmental Panel on Climate Change. In: Press CU, editor. Cambridge, United Kingdom and New York, NY, USA.2014.
[3] IEA. Energy Eficiency 2019. In: Agency IE, editor. Paris, France2019.
[4] Attia S, Hamdy M, O'Brien W, Carlucci S. Assessing gaps and needs for integrating building performance optimization tools in net zero energy buildings design. Energy and Buildings. 2013;60(0):110-24.
[5] Nguyen A-T, Reiter S, Rigo P. A review on simulation-based optimization methods applied to building performance analysis. Applied Energy. 2014;113(0):1043-58.
[6] Amasyali K, El-Gohary NM. A review of data-driven building energy consumption prediction studies. Renewable and Sustainable Energy Reviews. 2018;81:1192-205.
[7] Westermann P, Evins R. Surrogate modelling for sustainable building design – A review. Energy and Buildings. 2019;198:170-86.
[8] Barreiro E, Munteanu CR, Cruz-Monteagudo M, Pazos A, González-Díaz H. Net-Net Auto Machine Learning (AutoML) Prediction of Complex Ecosystems. Scientific Reports. 2018;8(1):12340.
[9] Feurer M, Klein A, Eggensperger K, Springenberg JT, Blum M, Hutter F. Auto-sklearn: Efficient and Robust Automated Machine Learning. In: Hutter F, Kotthoff L, Vanschoren J, editors. Automated Machine Learning: Methods, Systems, Challenges. Cham: Springer International Publishing; 2019. p. 113-34.
[10] Hepbasli A. Low exergy (LowEx) heating and cooling systems for sustainable buildings and societies. Renewable and Sustainable Energy Reviews. 2012;16(1):73-104.
[11] García Kerdan I, Raslan R, Ruyssevelt P, Morillón Gálvez D. A comparison of an energy/economic-based against an exergoeconomic-based multi-objective optimisation for low carbon building energy design. Energy. 2017;128:244-63.
[12] Dincer I. The role of exergy in energy policy making. Energy Policy. 2002;30(2):137-49.
[13] Streich M. Opportunities and limits for exergy analysis in cryogenics. Chemical Engineering & Technology. 1996;19(6):498-502.
[14] Montelongo-Luna JM, Svrcek WY, Young BR. An exergy calculator tool for process simulation. Asia-Pacific Journal of Chemical Engineering. 2007;2(5):431-7.
[15] Querol E, Gonzalez-Regueral B, Ramos A, Perez-Benedito JL. Novel application for exergy and thermoeconomic analysis of processes simulated with Aspen Plus®. Energy. 2011;36(2):964-74.
[16] Ishida M, Zheng D, Akehata T. Evaluation of a chemical-looping-combustion power-generation system by graphic exergy analysis. Energy. 1987;12(2):147-54.
[17] Kaşka Ö. Energy and exergy analysis of an organic Rankine for power generation from waste heat recovery in steel industry. Energy Conversion and Management. 2014;77:108-17.
[18] Dincer I, Zamfirescu C. Sustainable Energy Systems and Applications. US: Springer 2012.
[19] Gasparatos A, El-Haram M, Horner M. Assessing the sustainability of the UK society using thermodynamic concepts: Part 2. Renewable and Sustainable Energy Reviews. 2009;13(5):956-70.
[20] ECB-Annex49. Detailed Exergy Assessment Guidebook for the Built Environment, IEA ECBCS. In: Torio H, Schmidt D, editors.: Fraunhofer IBP; 2011.

[21] Ala-Juusela M, Angelotti A, Koroneos C, Van der Kooi HJ, Simone A, Olesen BW. Low-exergy in the built environment insights from the costeXergy action 2007-2012 In: Technology CECiSa, editor.2014.
[22] Fisk D. Optimising heating system structure using exergy Branch and Bound. Building Services Engineering Research and Technology. 2014;35(3):321-33.
[23] García Kerdan I, Raslan R, Ruyssevelt P, Vaiciulyte S, Morillón Gálvez D. Thermodynamic and exergoeconomic analysis of a non-domestic Passivhaus retrofit. Building and Environment. 2017;117:100-17.
[24] Shadram F, Bhattacharjee S, Lidelöw S, Mukkavaara J, Olofsson T. Exploring the trade-off in life cycle energy of building retrofit through optimization. Applied Energy. 2020;269:115083.
[25] Geyer P, Singaravel S. Component-based machine learning for performance prediction in building design. Applied Energy. 2018;228:1439-53.
[26] Melo AP, Cóstola D, Lamberts R, Hensen JLM. Development of surrogate models using artificial neural network for building shell energy labelling. Energy Policy. 2014;69:457-66.
[27] Hashempour N, Taherkhani R, Mahdikhani M. Energy performance optimization of existing buildings: A literature review. Sustainable Cities and Society. 2020;54:101967.
[28] Wortmann T, Costa A, Nannicini G, Schroepfer T. Advantages of surrogate models for architectural design optimization. Artificial Intelligence for Engineering Design, Analysis and Manufacturing. 2015;29(4):471-81.
[29] Korolija I, Marjanovic-Halburd L, Zhang Y, Hanby VI. UK office buildings archetypal model as methodological approach in development of regression models for predicting building energy consumption from heating and cooling demands. Energy and Buildings. 2013;60(0):152-62.
[30] Edwards RE, New J, Parker LE, Cui B, Dong J. Constructing large scale surrogate models from big data and artificial intelligence. Applied Energy. 2017;202:685-99.
[31] Bornatico R, Hüssy J, Witzig A, Guzzella L. Surrogate modeling for the fast optimization of energy systems. Energy. 2013;57:653-62.
[32] Chen X, Yang H. Integrated energy performance optimization of a passively designed high-rise residential building in different climatic zones of China. Applied Energy. 2018;215:145-58.
[33] Widrow B. An adaptive "Adaline" neuron using chemical "memistors". In: Research OoN, editor. Stanford, California: Solid-State Electronics Laboratory, Stanford University; 1960.
[34] Hagan MT, Demuth HB, Beale M. Neural Network Design. Conference Neural Network Design.
[35] Kalogirou SA. Applications of artificial neural-networks for energy systems. Applied Energy. 2000;67(1):17-35.
[36] Magnier L, Haghighat F. Multiobjective optimization of building design using TRNSYS simulations, genetic algorithm, and Artificial Neural Network. Building and Environment. 2010;45(3):739-46.
[37] Wong SL, Wan KKW, Lam TNT. Artificial neural networks for energy analysis of office buildings with daylighting. Applied Energy. 2010;87(2):551-7.
[38] Ascione F, Bianco N, De Stasio C, Mauro GM, Vanoli GP. Artificial neural networks to predict energy performance and retrofit scenarios for any member of a building category: A novel approach. Energy. 2017;118:999-1017.
[39] del Rio-Chanona EA, Wagner JL, Ali H, Fiorelli F, Zhang D, Hellgardt K. Deep learning-based surrogate modeling and optimization for microalgal biofuel production and photobioreactor design. AIChE Journal. 2019;65(3):915-23.
[40] Sharif SA, Hammad A. Developing surrogate ANN for selecting near-optimal building energy renovation methods considering energy consumption, LCC and LCA. Journal of Building Engineering. 2019;25:100790.
[41] Sözen A, Arcaklioğlu E. Exergy analysis of an ejector-absorption heat transformer using artificial neural network approach. Applied Thermal Engineering. 2007;27(2):481-91.
[42] Yoru Y, Karakoc TH, Hepbasli A. Application of Artificial Neural Network (ANN) Method to Exergy Analysis of Thermodynamic Systems. Conference Application of Artificial Neural Network (ANN) Method to Exergy Analysis of Thermodynamic Systems. p. 715-8.

[43] Khosravi A, Syri S, Zhao X, Assad MEH. An artificial intelligence approach for thermodynamic modeling of geothermal based-organic Rankine cycle equipped with solar system. Geothermics. 2019;80:138-54.
[44] Aghbashlo M, Shamshirband S, Tabatabaei M, Yee PL, Larimi YN. The use of ELM-WT (extreme learning machine with wavelet transform algorithm) to predict exergetic performance of a DI diesel engine running on diesel/biodiesel blends containing polymer waste. Energy. 2016;94:443-56.
[45] Yang L, Nagy Z, Goffin P, Schlueter A. Reinforcement learning for optimal control of low exergy buildings. Applied Energy. 2015;156:577-86.
[46] Koopialipoor M, Jahed Armaghani D, Haghighi M, Ghaleini EN. A neuro-genetic predictive model to approximate overbreak induced by drilling and blasting operation in tunnels. Bulletin of Engineering Geology and the Environment. 2019;78(2):981-90.
[47] Azimi Y, Khoshrou SH, Osanloo M. Prediction of blast induced ground vibration (BIGV) of quarry mining using hybrid genetic algorithm optimized artificial neural network. Measurement. 2019;147:106874.
[48] Taghavi M, Gharehghani A, Nejad FB, Mirsalim M. Developing a model to predict the start of combustion in HCCI engine using ANN-GA approach. Energy Conversion and Management. 2019;195:57-69.
[49] Suresh MVJJ, Reddy KS, Kolar AK. ANN-GA based optimization of a high ash coal-fired supercritical power plant. Applied Energy. 2011;88(12):4867-73.
[50] Baklacioglu T, Turan O, Aydin H. Dynamic modeling of exergy efficiency of turboprop engine components using hybrid genetic algorithm-artificial neural networks. Energy. 2015;86:709-21.
[51] García Kerdan I, Raslan R, Ruyssevelt P, Morillón Gálvez D. ExRET-Opt: An automated exergy/exergoeconomic simulation framework for building energy retrofit analysis and design optimisation. Applied Energy. 2017;192:33-58.
[52] EnergyPlus. Getting Started with EnergyPlus. BasicConcepts Manual - Essential Information You Need about Running EnergyPlus. The Board of Trustees of the University of Illinois and the Regents of the University of California through the Ernest Orlando Lawrence Berkeley National Laboratory. 2012:73.
[53] García Kerdan I, Raslan R, Ruyssevelt P, Morillón Gálvez D. An exergoeconomic-based parametric study to examine the effects of active and passive energy retrofit strategies for buildings. Energy and Buildings. 2016;133:155-71.
[54] García Kerdan I, Morillón Gálvez D, Sousa G, Suárez de la Fuente S, Silva R, Hawkes A. Thermodynamic and thermal comfort optimisation of a coastal social house considering the influence of the thermal breeze. Building and Environment. 2019;155:224-46.
[55] García Kerdan I, Raslan R, Ruyssevelt P. An exergy-based multi-objective optimisation model for energy retrofit strategies in non-domestic buildings. Energy. 2016;117, Part 2:506-22.
[56] Pout CH. Proposed Carbon Emission Factors and Primary Energy Factors for SAP 2012. In: BRE, editor. Techical papers supporting SAP 2012. UK2011.
[57] Torío H, Angelotti A, Schmidt D. Exergy analysis of renewable energy-based climatisation systems for buildings: A critical view. Energy and Buildings. 2009;41(3):248-71.
[58] Fanger PO. Assessment of man's thermal comfort in practice. British Journal of Industrial Medicine. 1973;30(4):313.
[59] BSI. ISO 7730: Ergonomics of the Thermal Environment Analytical Determination and Interpretation of Thermal Comfort Using Calculation of the PMV and PPD Indices and Local Thermal Comfort Criteria. Geneva, Switzerland: ISO; 2005.
[60] ASHRAE. ANSI/ASHRAE Standard 55-2004. Thermal Environmental Conditions for Human Occupancy. American Society of Heating, Refrigerating and Air-conditioning Engineers; 2004.
[61] Abadi MaB, Paul and Chen, Jianmin and Chen, Zhifeng and Davis, Andy and Dean, Jeffrey and Devin, Matthieu and Ghemawat, Sanjay and Irving, Geoffrey and Isard, Michael and others. Tensorflow: A system for large-scale machine learning. 12th Symposium on Operating Systems Design and Implementation (OSDI16)2016. p. 265--83.

[62] Chollet Fao. Keras. https://keras.io2015.
[63] Deb K, Pratap A, Agarwal S, Meyarivan T. A fast and elitist multiobjective genetic algorithm: NSGA-II. IEEE Transactions on Evolutionary Computation. 2002;6(2):182-97.
[64] Yang M-D, Chen Y-P, Lin Y-H, Ho Y-F, Lin J-Y. Multiobjective optimization using nondominated sorting genetic algorithm-II for allocation of energy conservation and renewable energy facilities in a campus. Energy and Buildings. 2016;122:120-30.
[65] Perera ATD, Wickramasinghe PU, Nik VM, Scartezzini J-L. Machine learning methods to assist energy system optimization. Applied Energy. 2019;243:191-205.
[66] Python_Software_Foundation. Python Language Reference version 2.7.
[67] Garbin C, Zhu X, Marques O. Dropout vs. batch normalization: an empirical study of their impact to deep learning. Multimedia Tools and Applications. 2020;79(19):12777-815.

Appendices

Appendix A. Building technologies technoeconomic database

Table A-1 baseline model main characteristics [54]

Characteristic	Description
Total floor space (m^2)	130 (65 m^2 per flat)
Infiltration rate (ach)	4.0
Exterior Walls	Cavity Wall-Brick walls 130 mm brick with 20 mm air gap U_{value}= 0.72 W/m^2K
Roof	160 mm concrete block U_{value}= 3.93 W/m^2K
Ground floor	100 mm concrete slab U_{value}= 3.87 W/m^2K
Windows	Single-pane clear glass (5mm thick) U_{value}= 5.8 W/m^2K
Glazing ratio	15%
HVAC System	Minisplit system 5 kW and η= 90% No heating system
Cooling Set Point (°C)	22.5
Occupancy (people)	3-4 per flat
Equipment (W/m^2)	3.9
Lighting level (W/m^2)	10.7

Appendix B. Hyperparameters fitness evaluation

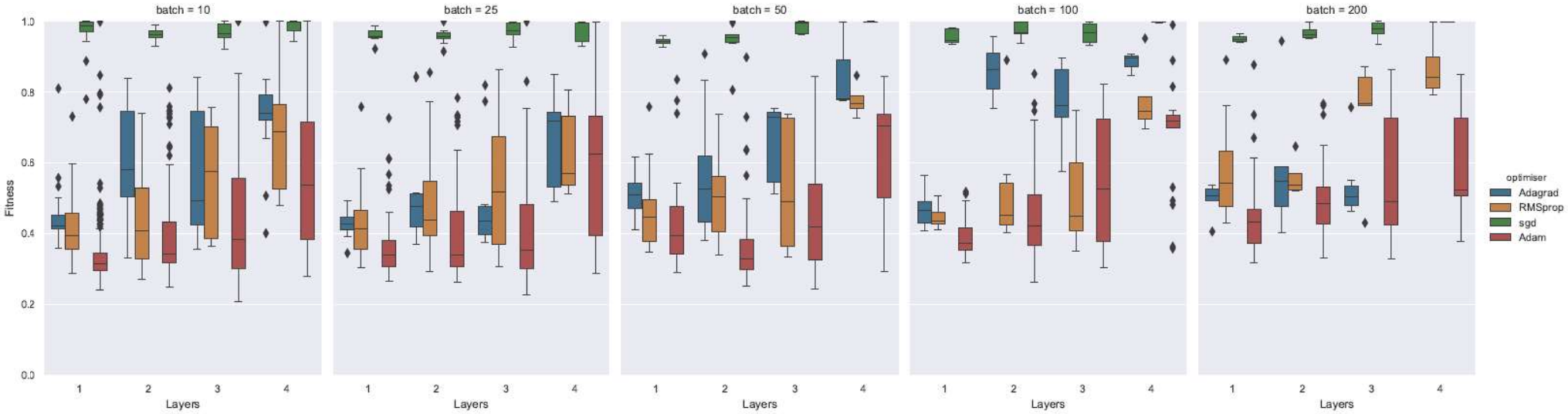

Fig. B-1 Batch sizes hyperparameter fitness evaluation

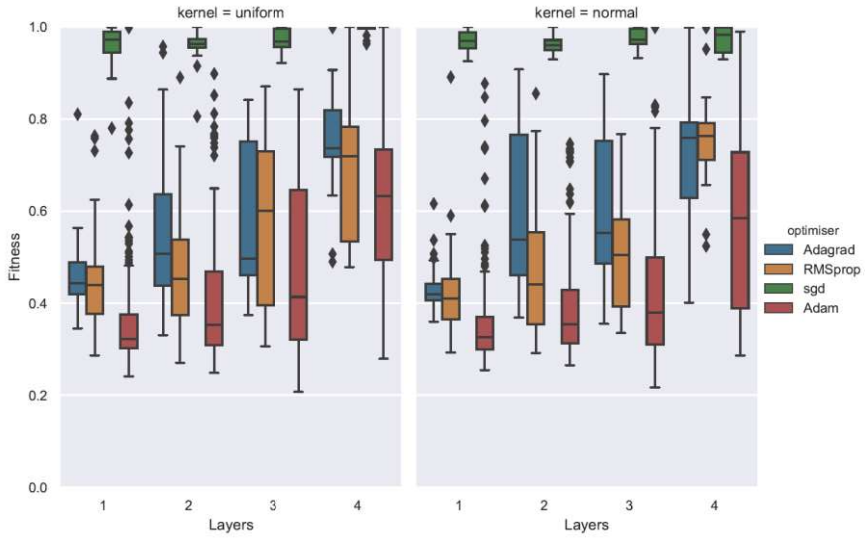

Fig. B-2 Kernel /weight initialiser hyperparameter fitness evaluation

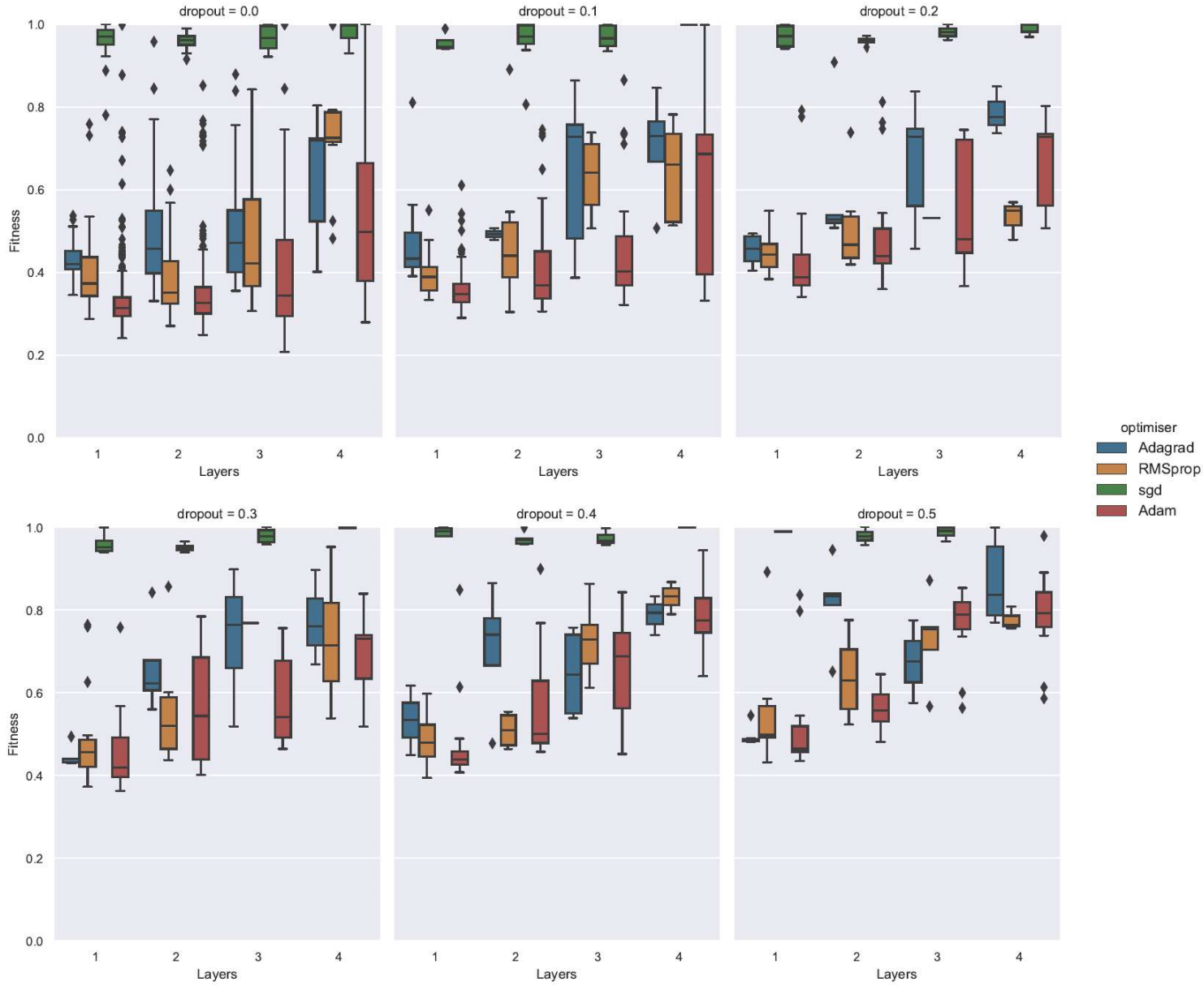

Fig. B-3 Dropout rate hyperparameter fitness evaluation

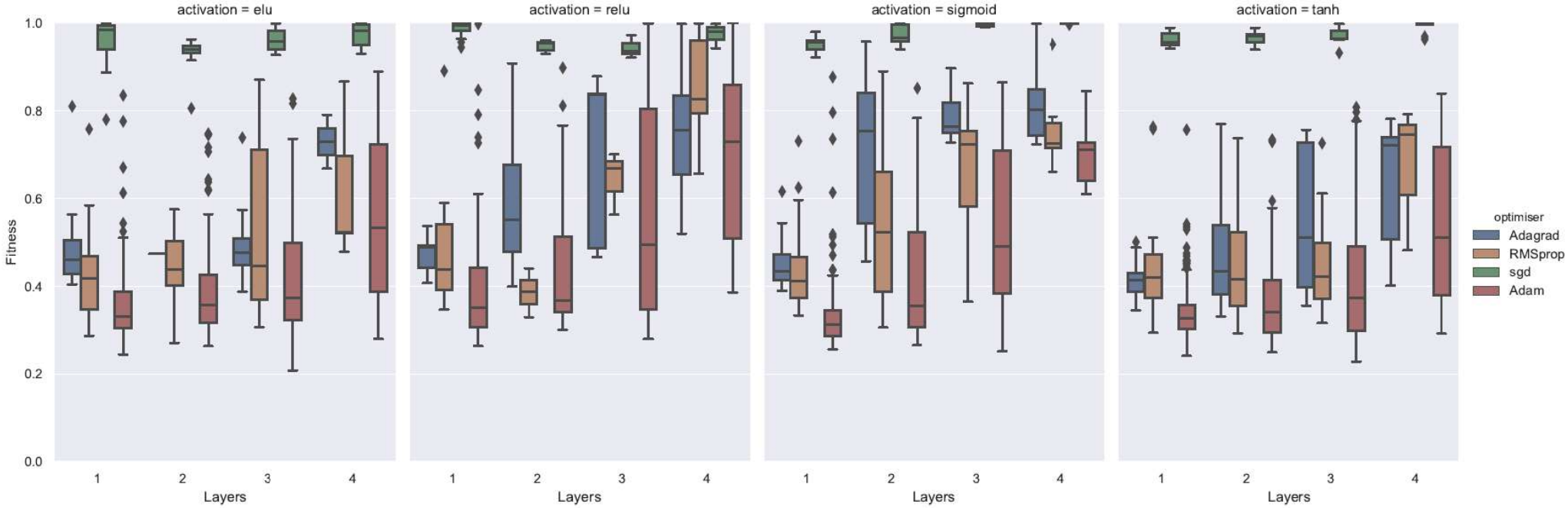

Fig. B-4 Activation function hyperparameter fitness evaluation

Appendix C. ANN performance validation

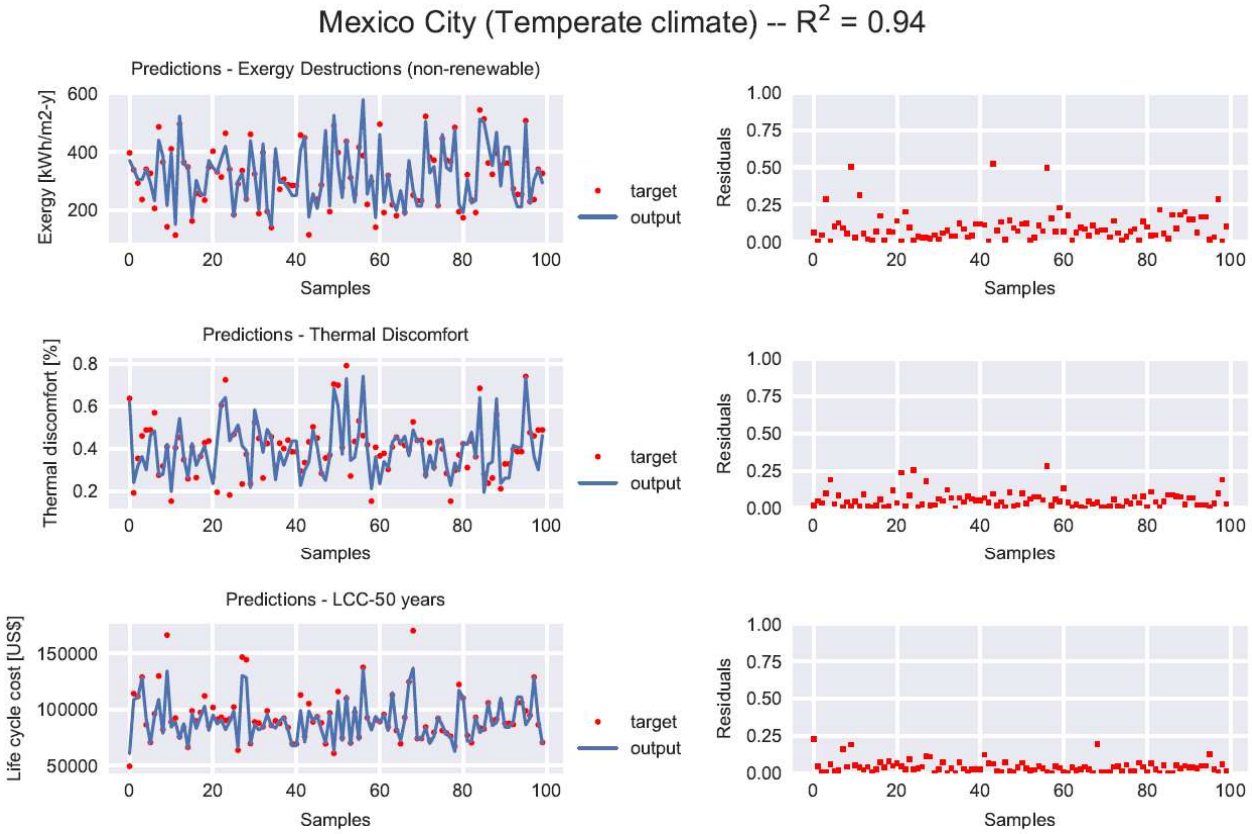

Fig. C-1 Optimal ANN model prediction performance and residuals for exergy, comfort and LCC in temperate climatic conditions

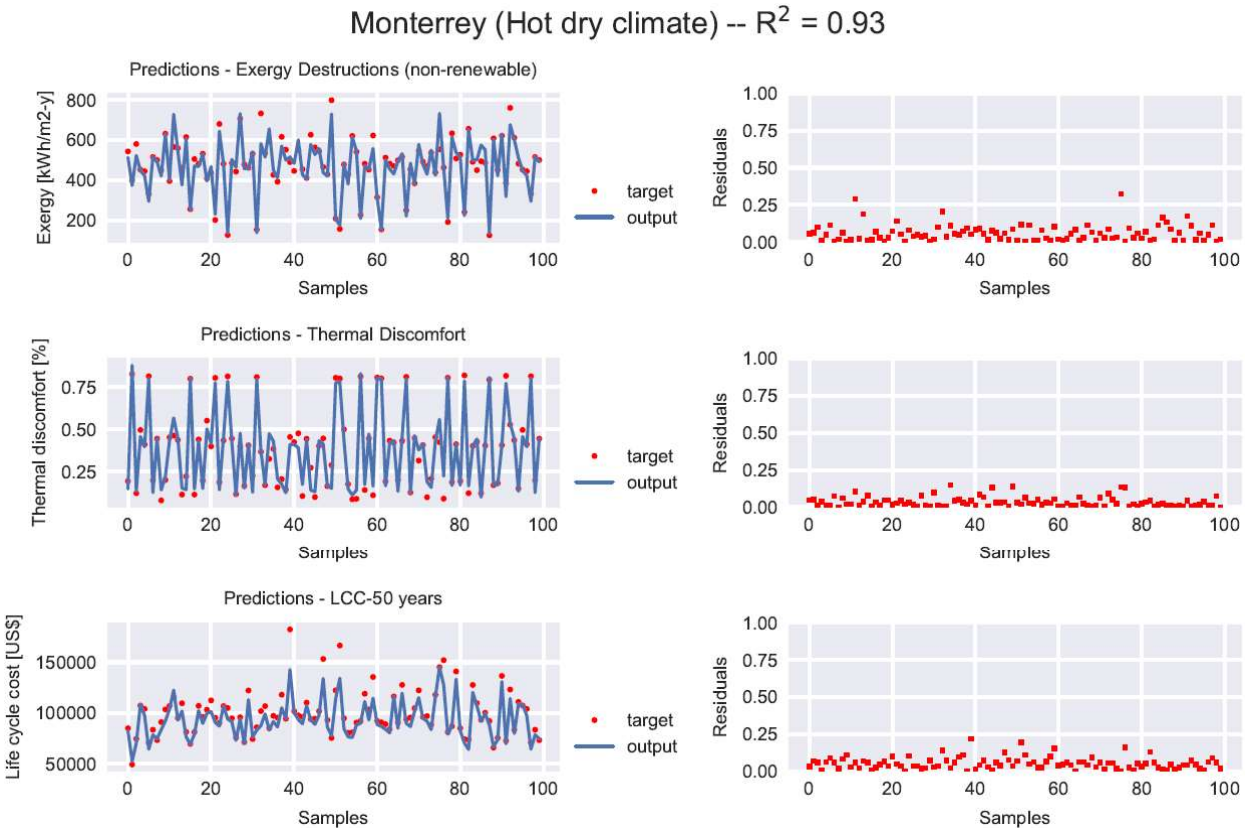

Fig. C-2 Optimal ANN model prediction performance and residuals for exergy, comfort and LCC in hot dry climatic conditions